

Manuscript No.: **acp-2016-764**

Journal: **ACP**

The revised manuscript entitled “**Comparison of key absorption and optical properties between pure and transported anthropogenic dust over East and Central Asia.**” by Jianrong Bi, et al.

**Response to Reviewer#1:**

We greatly appreciated for Editor’s big help! We have carefully checked and revised the manuscript according to Reviewers’ comments, which are helpful and valuable for greatly improving our manuscript. Please find a point-by-point reply to the issues as follows (highlighted in blue color font). And we have also uploaded the file of “Response to-Reviewer#1(acp-2016-764).pdf”.

**Suggestion:**

1. How to distinguish and separate the natural and anthropogenic contributions for climate variability, has become one of the most intractable problems in current global climate change. The authors proposed two threshold criteria to identify two types of Asian dust: Pure Dust (PDU,  $\alpha < 0.2$ ) and Transported Anthropogenic Dust (TDU,  $0.2 < \alpha < 0.6$ ), and explore the key absorption and optical properties. These results are encouraging and helpful to update the essential parameters of Asian dust in current remote sensing applications and climate models. As mentioned in the manuscript, it is still a huge challenge to discriminate between natural and anthropogenic components of dust aerosols by using current technology, AERONET products or in-situ measurements. However, the reviewer encourages the authors to explore detailed morphology, mineralogy, and chemical compositions by means of in situ measurements, laboratory analysis, active and passive remote sensing methods (e.g., multi-wavelength lidar, AEROENT, MODIS) as well as model calculations in the future work.

⇒ The authors don’t need to response this.

**Response:** Thank you very much for Reviewer’s good suggestions. To fully elucidate exact optical properties of anthropogenic dust, we shall explore detailed morphology,

mineralogy, and chemical compositions by means of in situ measurements, laboratory analysis, active and passive remote sensing methods (e.g., multi-wavelength lidar, AEROENT, MODIS) as well as model calculations in our future work.

**Minor comments:**

1. **Abstract**, Page 2, line 54: “OPAC”

⇒ Change to “Optical Properties of Aerosols and Clouds (OPAC)”. When an abbreviation firstly appears in the manuscript, please give the full name.

**Response:** We have changed “OPAC” to “Optical Properties of Aerosols and Clouds (OPAC)” in Line 54 and corresponding places in the whole text.

2. Page 3, line 80: “are about 6 times larger than at 660 nm”

⇒ Change to “are about 6 times larger than that at 660 nm”

**Response:** We have changed to “are about 6 times larger than that at 660 nm” in Line 80.

3. Page 4, line 114: “theory calculation”

⇒ Change to “theoretical calculation”

**Response:** We have changed “theory calculation” to “theoretical calculation” in Line 114.

4. Page 8, line 209: “compared to”

⇒ Change to “compared with”

**Response:** We have changed “compared to” to “compared with” in Line 209.

5. Page 8, line 219: “literatures”

⇒ Change to “literature”

**Response:** We have changed “literatures” to “literature” in Line 219.

6. Page 9, line 247: “linked to”

⇒ Change to “linked with”

**Response:** We have changed “linked to” to “linked with” in Line 247.

7. Page 17, line 494: “PUD”

⇒ Change to “PDU”

**Response:** We have changed “PUD” to “PDU” in Line 494.

## **Response to Reviewer#2:**

We are grateful to the Editor and the anonymous Reviewer for their constructive and insightful comments. The comments of the Reviewers are helpful and valuable for greatly improving the manuscript. Please find a point-by-point reply to the issues as follows (highlighted in blue color font). And we have also uploaded the file of “Response to-Reviewer#2(acp-2016-764)-supplement.pdf”.

### **Specific comments:**

(1) Page 16, lines 471-473: “The main input parameters of spectral AOD, surface albedo, WVC, and columnar ozone amount are prescribed to same values (e.g., ...)”

⇒Please give the prescribed values of spectral AOD, surface albedo, WVC, and columnar ozone amount in the manuscript, which would be convenient for audience.

**Response:** Thank you very much for Reviewer’s insightful comments. We have presented the prescribed values of spectral AOD, surface albedo, WVC, and columnar ozone amount in Lines 471-473, “(e.g., 0.72, 0.30, 1.0 cm, and 300 DU for input AOD<sub>440</sub>, surface albedo, WVC, and ozone amount)”.

(2) Page 33, Figure 5(b): For Minqin and Dunhuang sites, the AOD<sub>440</sub> and  $r_{\text{coarse}}$  are shown for “-”, the authors may want to indicate the missing data. Please give the explanation in the context.

**Response:** Thank you very much for Reviewer’s good comments. We have added “Note that the “-” in Figure 5(b) represents that missing data for AOD<sub>440</sub> and  $r_{\text{coarse}}$  at Dunhuang and Minqin sites.” in Page 34, Lines 912-913.

### **Minor comments:**

(1) 1. Introduction, Page 5, line 142: Please add “There have been several world-famous aerosol long-term monitoring networks over Asian region for examining aerosol features and its radiative effects, for instance,

AERONET—AErosol RObotic NETwork (Holben et al., 1998), SKYNET—aerosol-cloud-radiation interaction ground-based observation network (Nakajima et al., 1996; Takamura et al., 2004; Che et al., 2008), and CARSNET—China Aerosol Remote Sensing Network (Che et al., 2009, 2014, 2015).” at the beginning of this section and add corresponding cited literature in References.

**Response:** We have added “There have been several world-famous aerosol long-term monitoring networks over Asian region for examining aerosol features and its radiative effects, for instance, AERONET—AErosol RObotic NETwork (Holben et al., 1998), SKYNET—aerosol-cloud-radiation interaction ground-based observation network (Nakajima et al., 1996; Takamura et al., 2004; Che et al., 2008), and CARSNET—China Aerosol Remote Sensing Network (Che et al., 2009a, 2014, 2015).” at the beginning of this section and add corresponding cited literature in References.

(2) Page 7, line 200: “**3. Asian Dust Optical properties**”

⇒ Change to “**3. Asian Dust Optical Properties**”

**Response:** We have changed to “**3. Asian Dust Optical Properties**” in Page 7, Line 200.

(3) Page 7, lines 201-205: Change to “A great amount of publications have verified that mineral dust aerosols are commonly predominant by large particles with coarse mode (radii>0.6 μm), which are the essential feature differentiating the dust from fine-mode dominated biomass burning and urban-industrial aerosols (Dubovik et al., 2002b; Eck et al., 2005; Bi et al., 2011, 2014; Kim et al., 2011; Che et al., 2013).”

**Response:** We have changed in Page 7, Lines 201-205.

(4) Page 8, line 209: “compared to”

⇒ Change to “compared with”

**Response:** We have changed “compared to” to “compared with” in Line 209.

(5) Page 8, line 219: change “literatures” to “literature” and modify the other places in the whole manuscript.

**Response:** We have changed “literatures” to “literature” in Line 219 and modify the

other places in the whole manuscript.

(6) Page 9, lines 259-260: “Note that the occurred months of PDU days are nearly different from TDU days at Dalanzadgad,”

⇒ Change to “Note that the occurred months of PDU cases are nearly different from TDU cases at Dalanzadgad,”

**Response:** We have changed to “Note that the occurred months of PDU cases are nearly different from TDU cases at Dalanzadgad,” in Page 9, Lines 259-260.

(7) Page 10, line 294: “and estimated SSA at 325 nm (~0.80) is much lower than at 660 nm (~0.95).”

⇒ Change to “and estimated SSA at 325 nm (~0.80) is much lower than that at 660 nm (~0.95).”

**Response:** We have changed “and estimated SSA at 325 nm (~0.80) is much lower than that at 660 nm (~0.95).” in Page 10, Line 294.

(8) 5. Summary, Page 17, line 494: change “PUD” to “PDU” and modify the other places in the whole manuscript.

**Response:** We have changed “PUD” to “PDU” in Page 17, Line 494 and modify the other places in the whole manuscript.

### **Anonymous Referee#3:**

The work presented in this paper is very interesting and well structured. The authors suggest a method for discriminating the presence of Desert dust in the atmosphere, dividing it into two different cases: pure dust and transported anthropogenic dust. The method is based on a threshold on AOD (440 nm) and Angstrom exponent (calculated using the two wavelengths 400 and 870 nm), and provided good results when compared with the plots of the volume size distributions. Also the section devoted to the comparison among the values retrieved from measurements and the ones from models generally used, is very interesting and useful.

### **Response to Referee#3:**

We are grateful to the Editor and the anonymous Referee for their constructive and insightful comments. The comments of the Referees are helpful and valuable for

greatly improving the manuscript. Please find a point-by-point reply to the issues as follows (highlighted in blue color font). And we have also uploaded the file of “Response to-Referee#3(acp-2016-764)-supplement.pdf”.

(2) To complete the paper, I suggest the authors to give a look to the following paper where a similar work has been done for Saharan dust in Europe: “Inventory of African desert dust events over the southwestern Iberian Peninsula in 2000-2005 with an AERONET Cimel Sun photometer”, Toledano et al., 2007, DOI:10.1029/2006JD008307. Also in this paper thresholds on Angstrom exponent and AOD are used in order to set up an Automatic Criterion for Detection and Evaluation of Desert Dust Intrusions and, as expected, they are different from the ones used in this paper. I think it should be highlighted in the text that the chosen values are good for the type of dust intrusion of the selected area, and that for a smaller area or a different geographical location, they must be selected carefully. In that paper it is also written that a larger sensitivity to the presence of dust particles has been found at 870 nm rather than 440 nm. Do the authors think that using a threshold on this wavelength in the case of TDU would help to discriminate more accurately the amount of dust from the anthropogenic aerosols? Did the author never found (in TDU dataset) a 3 modal volume size distribution? If yes, it could be another possibility for better understanding the composition of TDU dust.

**Response:** Thank you very much for Reviewer’s insightful comments. We have read carefully the paper of Toledano et al. [JGR, 2007]. In their Automatic Criterion for Detection and Evaluation of Desert Dust Intrusions, they mainly based on AOD and Angstrom exponent ( $AOD(870nm) > 0.11$  and  $\alpha < 0.99$ ), manual inspection, and volume concentrations (fine and coarse modes), and confirmation with back trajectories and satellite-constitute the basic methodology to establish the inventory of African dust events. As pointed out by Toledano et al., “In principle the criterion derived here for the detection of desert aerosol events is only valid for our site, that is, it is a local criterion.” (Page 11).

If we used the threshold on 870 nm wavelength ( $AOD(870nm) > 0.11$  and

alpha<0.99) to identify the TDU in our manuscript, we found that there were a lot of cases meet this condition, that is, both dust aerosols and the other aerosol types (e.g., urban-industrial aerosol) have got AOD(870nm)>0.11 and alpha<0.99. Therefore, we could not discriminate among the pure dust, TDU, and fine-mode dominated non-dust aerosols in our study. Meanwhile, we have checked the TDU datasets at all selected sites in our paper, we only found that there were only a few TDU cases (less than 1%) with a 3 modal volume size distribution. Anyway, we greatly appreciated the Referee's insightful comments, and we would bear in mind these good suggestions in our future work.

**Minor comments:**

(1) Line 189: put the acronyms of SSA, ASY, Ri and Re in line 186, where these quantities are listed.

**Response:** Thank you very much for Referee's good comments! We have presented the full name of SSA, ASY, Ri and Re in Lines 145-146, so we used the acronyms here.

(2) Line 192: "are dependent on AOD440>=0.4" I think it would be better saying "are valid for AOD440..."

**Response:** We have changed "are dependent on" to "are valid for" in Line 192.

(3) Line 277: "capability" instead of "intensity"

**Response:** We have changed "capability" to "intensity" in Line 277.

(4) Line 346: it is written that the pick radius of the coarse mode is about 2.24 for both PDU and TDU. However for Yulin in TDU it seems to be about 3. I think that in the case of TDU it would be better saying that the pick radius in between 2-3 um.

**Response:** Thank you very much for Referee's insightful comments! The  $r_{vc}$  of TDU cases actually vary between 2 to 3  $\mu\text{m}$ . So, we have changed "for all PDU and TDU cases" to "for all PDU cases and  $r_{vc}\sim 2.0\text{-}3.0\ \mu\text{m}$  for TDU cases" in Line 346.

(5) Lines 512-514: the sentence begins with "because" but it doesn't seem to have a correct grammatical structure (subject, verb, object...). Please check it.

**Response:** We have deleted "because" and changed to "It is very difficult to quantify

the anthropogenic contribution due to large uncertainties in defining...” in Lines 512-514.



1 **Comparison of key absorption and optical properties between pure**  
2 **and transported anthropogenic dust over East and Central Asia**

3 Jianrong Bi<sup>1</sup>, Jianping Huang<sup>1\*</sup>, Brent Holben<sup>2</sup>, Guolong Zhang<sup>1</sup>

4

5 <sup>1</sup>Key Laboratory for Semi-Arid Climate Change of the Ministry of Education, College of  
6 Atmospheric Sciences, Lanzhou University, Lanzhou, 730000, China

7 <sup>2</sup>NASA Goddard Space Flight Center, Greenbelt, Maryland, USA

8

9 *Submitted to: ACP Special Issue*

10

11

12

13

14

15

16

17

18

19

20

21

22

23

24

25

26

27

-----

28 *\*Correspondence to: Jianping Huang (hjp@lzu.edu.cn)*

29

30 **Abstract.** Asian dust particulate is one of the primary aerosol constituents in the  
31 Earth-atmosphere system that exerts profound influences on environmental quality,  
32 human health, marine biogeochemical cycle and Earth's climate. To date, the  
33 absorptive capacity of dust aerosol generated from Asian desert region is still an open  
34 question. In this article, we compile columnar key absorption and optical properties of  
35 mineral dust over East and Central Asia areas by utilizing the multi-year quality  
36 assured datasets observed at 13 sites of the Aerosol Robotic Network (AERONET).  
37 We identify two types of Asian dust according to threshold criteria from previously  
38 published literature. (I) The particles with high aerosol optical depth at 440 nm  
39 ( $AOD_{440} \geq 0.4$ ) and low Ångström wavelength exponent at 440-870 nm ( $\alpha < 0.2$ ) are  
40 defined as Pure Dust (PDU) that decrease disturbance of other non-dust aerosols and  
41 keep high accuracy of pure Asian dust. (II) The particles with  $AOD_{440} \geq 0.4$  and  
42  $0.2 < \alpha < 0.6$  are designated as Transported Anthropogenic Dust (TDU), which are  
43 mainly dominated by dust aerosol and might mix with other anthropogenic aerosol  
44 types. Our results reveal that the primary components of high AOD days are  
45 predominant by dust over East and Central Asia regions even if their variations rely  
46 on different sources, distance from the source, emission mechanisms, and  
47 meteorological characteristics. The overall mean and standard deviation of  
48 single-scattering albedo, asymmetry factor, real part and imaginary part of complex  
49 refractive index at 550 nm for Asian PDU are  $0.935 \pm 0.014$ ,  $0.742 \pm 0.008$ ,  
50  $1.526 \pm 0.029$ ,  $0.00226 \pm 0.00056$ , respectively, while corresponding values are  
51  $0.921 \pm 0.021$ ,  $0.723 \pm 0.009$ ,  $1.521 \pm 0.025$ , and  $0.00364 \pm 0.0014$  for Asian TDU.  
52 Aerosol shortwave direct radiative effects at the top of the atmosphere (TOA), at the  
53 surface (SFC), and in the atmospheric layer (ATM) for Asian PDU ( $\alpha < 0.2$ ) and TDU  
54 ( $0.2 < \alpha < 0.6$ ) computed in this study, are a factor of 2 smaller than the results of  
55 [Optical Properties of Aerosols and Clouds \(OPAC\)](#) Mineral accumulated  
56 (Mineral acc.) and transported (Mineral tran.) modes. Therefore, we are convinced  
57 that our results hold promise of updating and improving accuracies of Asian dust  
58 characteristics in present-day remote sensing applications and regional or global

59 climate models.

## 60 **1. Introduction**

61 Airborne dust particle (also called mineral dust) is recognized as one of the most  
62 important aerosol species in the tropospheric atmosphere, which accounts for about  
63 30% of the total aerosol loading and extinction aerosol optical depth on a global scale  
64 (Perlwitz et al., 2001; Kinne et al., 2006; Chin et al., 2009; Huang et al., 2014). High  
65 concentrations of dust aerosols hanging over desert source regions and invasive  
66 downstream areas would seriously exacerbate air quality, degrade visibility, affect  
67 transportation safety, and do adverse effects on public health during the prevalent  
68 seasons of dust storms (Chan et al., 2008; Morman and Plumlee, 2013; Wang et al.,  
69 2016). When mineral dusts are deposited onto the Earth's surface, they play a key role  
70 in biogeochemical cycles of terrestrial ecosystem or ocean (Okin et al., 2004; Jickells  
71 et al., 2005; Shao et al., 2011), as well as alter snow and ice albedo (Aoki et al., 2006;  
72 Huang et al., 2011; Wang et al., 2014). Last but not least, dust particles can modulate  
73 the Earth's energy budget and drive the climate change directly by scattering and  
74 absorption of solar/terrestrial radiation (Charlson et al., 1992; Wang et al., 2010b;  
75 Huang et al., 2014), and indirectly by acting as effective cloud condensation nuclei or  
76 ice nuclei, influencing the cloud microphysics and precipitation processes  
77 (Ramanathan et al., 2001; Rosenfeld et al., 2001; DeMott et al., 2003; Huang et al.,  
78 2005, 2006, 2010a; Wang et al., 2010c; Creamean et al., 2013). Numerous studies  
79 (Sokolik and Toon, 1999; Lafon et al., 2004, 2006) have confirmed that dust particle  
80 is one kind of light absorbing substances, and its mass absorption efficiencies at 325  
81 nm (0.06~0.12 m<sup>2</sup>/g) are about 6 times larger than that at 660 nm (0.01~0.02 m<sup>2</sup>/g),  
82 owing to the greater absorbing potential of iron oxides at short wavelengths (Alfaro et  
83 al., 2004). However, the way of iron oxides mixed with quartz or clay is complicated  
84 and strongly impacts the resulting absorption (Claquin et al., 1998, 1999; Sokolik and  
85 Toon, 1999). And these mineralogical studies indicate that a lack of consideration of  
86 these mixing mechanisms is a significant limitation of the previous dust absorption  
87 computations. Although the absorptive ability of dust is two orders of magnitude

88 lower than for black carbon (Yang et al., 2009), the atmospheric mass loading of the  
89 former is the same magnitude larger than that of the latter, leading to the total  
90 absorption in solar spectrum comparable to black carbon. Chin et al. (2009) evaluated  
91 that dust may account for about 53% of global averaged aerosol absorption optical  
92 depth at 550 nm, which undoubtedly changes the aforementioned  
93 dust-cloud-precipitation interaction and exerts a significant effect on hydrological  
94 cycle of the Earth-atmosphere system.

95 East and Central Asia territories are the major source regions of dust aerosols on  
96 Earth, which produce a large amount of dust particles every year that become  
97 entrained into the upper atmosphere by cold fronts (Zhang et al., 1997; Huang et al.,  
98 2009, 2010a, 2014). They can travel over thousands of kilometers, even across the  
99 Pacific Ocean and reach the western coast of North America about one week with the  
100 prevailing westerly wind (Husar et al., 2001; Uno et al., 2009, 2011), and then modify  
101 the climate and environment over extensive area of Asia-Pacific rim. Thus far, there  
102 have been a great deal of fruitful field campaigns for exploring Asian dust (e.g.,  
103 U.S.S.R.-U.S., ACE-Asia, ADEC, PACDEX, EAST-AIRC), however, most focus on  
104 intensive observation period (Golitsyn and Gillette, 1993; Huebert et al., 2003;  
105 Nakajima et al., 2003; Mikami et al., 2006; Huang et al., 2008a; Li et al., 2011) and  
106 lack of long-term and quantitative knowledge of dust optical, microphysical  
107 characteristics (especially absorption properties) and chemical compositions over  
108 these regions. Hence, the absorptive capacity of Asian dust aerosol is still an  
109 outstanding issue. The variations of dust optical features in model calculations are  
110 closely related to the uncertainties in particle size distribution and prescribing a value  
111 for complex refractive index. Whereas the key parameters of Asian dust aerosols in  
112 present-day climate models are still prescribed to the predetermined properties of  
113 Saharan mineral dust.

114 Wang et al. (2004) inferred the refractive index of pure minerals at Qira in  
115 Taklimakan Desert during April 12-14, 2002 via combination of ~~theoretical~~  
116 calculation and composition analysis of aerosol samples, and showed that the value of  
117 imaginary part is 0.00411 at 500 nm, which is consistent with the Central Asian dust

118 of  $0.004 \pm 0.001$  (Tadzhikistan Desert; Sokolik and Golitsyn, 1993). Uchiyama et al.  
119 (2005) determined the single-scattering albedo (SSA) of Aeolian dust from sky  
120 radiometer and in situ measurements, and concluded that unpolluted Aeolian dust  
121 (source from Taklimakan Desert) has low absorption (with  $SSA_{500}$  of  $0.93 \sim 0.97$ ). Kim  
122 et al. (2004) analyzed multiyear sky radiation measurements over East Asian sites of  
123 Skyradiometer Network (Nakajima et al., 1996; Takamura et al., 2004) and showed  
124 the  $SSA_{500}$  of dust particles are around 0.9 in arid Dunhuang of northwest China and  
125 Mandalgovi Gobi desert in Mongolia. Bi et al. (2014) also reported the similar  $SSA_{550}$   
126 ( $0.91 \sim 0.97$ ) of dust aerosol at Dunhuang during spring of 2012. Xu et al. (2004)  
127 gained  $SSA_{530}$  of  $0.95 \pm 0.05$  in Yulin, China, from a Radiance Research nephelometer  
128 and a Particle Soot Absorption Photometer (PSAP) and suggested that both desert dust  
129 and local pollution sources contributed to the aerosol loading in Yulin during April  
130 2001. Whereas Ge et al. (2010) examined dust aerosol optical properties at Zhangye  
131 (a semiarid area of northwest China) from multifilter rotating shadowband radiometer  
132 (MFRSR) during spring of 2008 and found that although there are low aerosol optical  
133 depth values ( $AOD_{670}$  ranging from  $0.07 \sim 0.25$ ), dust particles have strong absorption  
134 (with  $SSA_{500}$  of  $0.75 \pm 0.02$ ) due to mixing with local anthropogenic pollutants. This  
135 result is close to the New Delhi over India ( $0.74 \sim 0.84$  for  $SSA_{500}$ ; Pandithurai et al.,  
136 2008). Lafon et al. (2006) revealed that due to containing of less calcite and higher  
137 fraction of iron oxide-clay aggregates, mineral dusts in Niger (Banizoumbou,  $13^{\circ}31'N$ ,  
138  $2^{\circ}38'E$ ) have much lower SSA in the visible wavelengths than that of Chinese (Ulan  
139 Buh,  $39^{\circ}26'N$ ,  $105^{\circ}40'E$ ) and Tunisian (Maouna,  $33^{\circ}01'N$ ,  $10^{\circ}40'E$ ) desert locations.  
140 Therefore, complete clarification of the climate-relevant impacts of Asian dust  
141 aerosols requires extensive and long-term measurements of the optical, microphysical  
142 and chemical properties, along with their spatial and temporal distributions.

143 There have been several world-famous aerosol long-term monitoring networks  
144 over Asian region for examining aerosol features and its radiative effects, for instance,  
145 AERONET—Aerosol RObotic NETwork (Holben et al., 1998),  
146 SKYNET—aerosol-cloud-radiation interaction ground-based observation network  
147 (Nakajima et al., 1996; Takamura et al., 2004; Che et al., 2008), and

148 | [CARSNET—China Aerosol Remote Sensing Network \(Che et al., 2009a, 2014, 2015\).](#)

149 | In this paper, we investigate optical characteristics of Asian dust from multi-year  
150 | ~~Aerosol RObotic NETwork~~ (AERONET) measurements at 13 sites in and around arid  
151 | or semi-arid regions of East and Central Asian desert sources. The key quantities  
152 | include single-scattering albedo (SSA), asymmetry factor (ASY), real part (Re) and  
153 | imaginary part (Ri) of complex refractive index, volume size distribution (dV/dlnr),  
154 | which are needed for climate simulating and remote sensing applications. We mainly  
155 | compare the vital absorption and optical properties between pure and transported  
156 | anthropogenic dust over East and Central Asia. This article is arranged as follows.  
157 | Section 2 introduces the site description and measurement. The identification method  
158 | and detailed Asian dust optical features are described in Section 3. Discussion of  
159 | spectral absorption behaviors of different dust aerosol types are given in Section 4 and  
160 | followed by the Summary in Section 5.

## 161 | **2. Site Description and Measurement**

### 162 | **2.1. Site Description**

163 | In this article, we select 13 AERONET sites located in arid or semi-arid Asian  
164 | regions (see Fig. 1), which are recognized as the primarily active centre of dust storms.  
165 | These drylands are very sensitive to climate change and human activities and would  
166 | accelerate drought expansion by the end of twenty-first century (Zheng et al., 2009;  
167 | Huang et al., 2016). Eight sites over East Asian region are labeled with red colors, and  
168 | five sites over Central Asian area are labeled with blue colors. The major Great  
169 | deserts or Gobi deserts along with plateaus are marked with black font (e.g., Great  
170 | Gobi desert in Mongolia, Taklimakan Desert, Thar Desert, Karakum Desert, Tibetan  
171 | Plateau, Loess Plateau, and Iranian Plateau). In order to quantitatively explore  
172 | detailed spectral absorptive characteristics of dust aerosols over East and Central Asia,  
173 | we choose four East Asian sites (SACOL, Dalanzadgad, Beijing, and Yulin) and four  
174 | Central Asian sites (Dushanbe, Karachi, Kandahar, and IASBS). They consist of:  
175 | SACOL located over Loess Plateau of northwest China (Huang et al., 2008b; Guan et  
176 | al., 2009; Huang et al., 2010b; Wang et al., 2010a), Dalanzadgad in the Great Gobi of

177 southern Mongolia (Eck et al., 2005), Beijing in the downwind of Inner Mongolia  
178 (Xia et al., 2007), Yulin on the southwestern fringe of the Mu Us desert in northwest  
179 China (Xu et al., 2004; Che et al., 2009**b**, 2015), Dushanbe in Tadjikistan situated at  
180 the transport corridor of Central Asian desert dust (i.e. Karakum Desert; Golitsyn and  
181 Gillette, 1993), Karachi located in the southern margin of Thar Desert in Pakistan and  
182 about 20 km from the east coast of Arabian Sea (Alam et al., 2011), Kandahar in the  
183 arid area of southern Afghanistan, IASBS on the Iranian Plateau of northwest Iran.

## 184 **2.2. Sun Photometer Measurements**

185 AERONET is an internationally federated global ground-based aerosol monitoring  
186 network utilizing Cimel sun photometer, which comprises more than 500 sites all over  
187 the world (Holben et al., 1998). The Cimel Electronique sun photometer (CE-318)  
188 takes measurements of sun direct irradiances at multiple discrete channels within the  
189 spectral range of 340-1640 nm, which can be calculated aerosol optical depth (AOD)  
190 and columnar water vapor content (WVC) in centimeter. Furthermore, the instrument  
191 can perform angular distribution of sky radiances at 440, 675, 870, and 1020 nm  
192 (nominal wavelengths), which can be simultaneously retrieved aerosol volume size  
193 distribution, complex refractive index, single-scattering albedo, and asymmetry factor  
194 under cloudless condition (Dubovik and King, 2000; Dubovik et al., 2002a, 2006).  
195 The total accuracy in AOD for a newly calibrated field instrument is about  
196 0.010-0.021 (Eck et al., 1999). The retrieval errors of SSA, ASY, Ri, and Re are  
197 anticipated to be 0.03-0.05, 0.04, 30%-50%, and 0.025-0.04, respectively, relying on  
198 aerosol types and loading (Dubovik et al., 2000). It should be borne in mind that these  
199 uncertainties are ~~valid for~~**dependent on**  $AOD_{440} \geq 0.4$  and for solar zenith angle  $>50^\circ$   
200 (Level 2.0 product), and the retrieval errors will become much greater when  $AOD_{440}$   
201  $<0.4$ . The datasets of selected 13 AERONET sites in this study come from the  
202 Level2.0 product, which are pre- and post-field calibrated, automatically cloud  
203 screened, and quality-assured (Smirnov et al., 2000). In addition, a mixture of  
204 randomly oriented polydisperse spheroid particle shape assumption with a fixed  
205 aspect ratio distribution is applied to retrieve key optical properties of Asian dust  
206 (Dubovik, et al., 2002a, 2006). Fu et al. (2009) have concluded that Mie-based

207 single-scattering properties of spheroidal dust aerosols are well suited in radiative flux  
208 calculations.

### 209 **3. Asian Dust Optical Properties~~properties~~**

210 A great amount of publications have verified that mineral dust aerosols are  
211 commonly predominant by large particles with coarse mode ( $\text{radii} > 0.6 \mu\text{m}$ ), which are  
212 the essential feature differentiating the dust from fine-mode dominated biomass  
213 burning and urban-industrial aerosols (Dubovik et al., 2002b; Eck et al., 2005; Bi et  
214 | al., 2011, 2014; Kim et al., 2011; Che et al., 2013). In other word, the values of  
215 Ångström exponent at 440-870 nm ( $\alpha$ ) for dust aerosols usually range between -0.1 to  
216 0.6. As pointed out by Smirnov et al. (2002) and Dubovik et al. (2002b), sea salt  
217 aerosol is also dominant by coarse mode and has small Ångström exponent ( $\sim 0.3-0.7$ )  
218 | but with low  $\text{AOD}_{440}$  ( $\sim 0.15-0.2$ ) compared with~~compared to~~ dust aerosol. Moreover,  
219 the selected desert locations in this study are mostly not affected by sea salt. By virtue  
220 of these differences, we can distinguish Asian dust aerosols from other fine-mode  
221 dominated non-dust particles. The criteria of two thresholds are put forward. (I) The  
222 particles with high aerosol optical depth at 440 nm ( $\text{AOD}_{440} \geq 0.4$ ) and low Ångström  
223 wavelength exponent at 440-870 nm ( $\alpha < 0.2$ ) are defined as Pure Dust (PDU) that  
224 keep high accuracy of pure Asian dust and eliminate most fine mode aerosols. (II) The  
225 particles with  $\text{AOD}_{440} \geq 0.4$  and  $0.2 < \alpha < 0.6$  are designated as Transported  
226 Anthropogenic Dust (TDU), which are mainly dominated by dust and might mix with  
227 other anthropogenic aerosol types during transportation. The definition of  
228 | anthropogenic dust in this study is different from earlier literature~~literatures~~ (Tegen  
229 and Fung, 1995; Prospero et al., 2002; Huang et al., 2015), which define that  
230 anthropogenic dust is primarily produced by various human activities on disturbed  
231 soils (e.g., agricultural practices, industrial activity, transportation, desertification and  
232 deforestation). It is still a huge challenge to discriminate between natural and  
233 anthropogenic components of dust aerosols by using current technology, AERONET  
234 products or in-situ measurements. Recently, Ginoux et al. (2012) first estimated that  
235 anthropogenic sources globally account for 25% based on Moderate Resolution



236 Imaging Spectroradiometer (MODIS) Deep Blue dust optical depth in conjunction  
237 with other land use data sets. Huang et al. (2015) proposed a new algorithm for  
238 distinguishing anthropogenic dust from natural dust by using Cloud-Aerosol Lidar  
239 and Infrared Pathfinder Satellite Observation (CALIPSO) and planetary boundary  
240 layer (PBL) height retrievals along with MODIS land cover data set. They revealed  
241 that anthropogenic dust produced by human activities mainly comes from semi-arid  
242 and semi-humid regions and is generally mixed with other types of aerosols within the  
243 PBL that is more spherical than natural dust. Thereby, we assume that anthropogenic  
244 dust aerosol originated from Asian arid or semi-arid areas has got smaller size  
245 distribution (thus larger Ångström exponent) than that of pure natural dust.

246 Before insight into dust aerosol optical characteristics, we first analyze the  
247 occurrence frequency of Asian dust over the study region that significantly affects the  
248 intensity and distribution of mineral dust loading. Figure 2 depicts the total number  
249 days of each month for Pure Dust ( $\alpha < 0.2$ ) and transported Anthropogenic Dust  
250 ( $0.2 < \alpha < 0.6$ ) at selected four East Asian sites and four Central Asian sites. The dust  
251 events at four East Asian sites primarily concentrate on springtime and corresponding  
252 peak days for PDU and TDU both appear in April. This is greatly attributed to the  
253 intrusion of dust particles during spring when dust storms are prevalent over these  
254 regions (Wang et al., 2008). For SACOL and Beijing sites, both the PDU and TDU  
255 days also occur in whole year except for autumn when is the rainy season, which is  
256 [linked with](#)~~linked to~~ long-range transport of dust particulates from desert source areas  
257 and locally anthropogenic dust (e.g., agricultural cultivation, overgrazing,  
258 desertification, industrial and constructed dust in urbanization). Shen et al. (2016)  
259 have demonstrated that urban fugitive dust generated by road transport and urban  
260 construction contributes to more than 70% of particulate matter (PM<sub>2.5</sub>) in northern  
261 China. The dust episodes in Dushanbe of Tadjikistan mostly happen from July to  
262 October, which are the peak seasons of dust storms (Golitsyn and Gillette, 1993). For  
263 Karachi site in Pakistan, the dust activities take place in spring and summer seasons.  
264 This is because the region is not affected by the summer monsoon, leaving the land  
265 surface sufficiently dry, and hence susceptible to wind erosion by strong winds and

266 meso-scale thunderstorm events typical of this time of year (Alizadeh Choobari et al.,  
267 2014). In addition, the transport of summer dust plumes from the Arabian Peninsula  
268 can partially contribute dust particles to Karachi site. Note that the occurred months of  
269 PDU cases are nearly different from TDU cases at Dalanzadgad~~Note that the occurred~~  
270 ~~months of PDU days are nearly different from TDU days at Dalanzadgad~~, Kandahar,  
271 and IASBS sites, suggesting that dust aerosols over these areas are rarely affected by  
272 anthropogenic pollutants. For Kandahar site in Afghanistan, the limited sampling days  
273 to some extent may affect the statistical results. Generally, the aforementioned  
274 occurrence frequency of dust storms over diverse sites are principally dependent on  
275 different climatic regime and synoptic pattern, for instance, geographical location,  
276 atmospheric circulation, wet season and dry season.

277 Table 1 summarizes the site information, sampling period, overall average optical  
278 properties at 550 nm (e.g., SSA, ASY, Re, Ri, and Ångström exponent at 440-870 nm)  
279 for Asian PDU ( $\alpha < 0.2$ ), and total number of PDU and TDU ( $0.2 < \alpha < 0.6$ ) days. Note  
280 that dust optical feature at a common 550 nm wavelength is utilized here, which can  
281 be derived from logarithmic interpolation between 440 and 675 nm. It is worth  
282 pointing out that the absorption and optical properties of dust aerosols at two  
283 Dunhuang sites exhibit consistent features despite of different sampling periods,  
284 which indicate that the chemical composition of dust aerosol at Dunhuang area  
285 remains relatively stable.

286 The SSA or Ri of complex refractive index can characterize the absorptive  
287 capability~~intensity~~ of dust aerosols, and determine the sign (cooling or heating,  
288 depending on the planetary albedo) of the radiative forcing (Hansen et al., 1997). Both  
289 two quantities are mainly relied on the ferric oxide content in mineral dust (Sokolik  
290 and Toon, 1999). Figure 3 illustrates the overall average spectral behavior of key  
291 optical properties for PDU ( $\alpha < 0.2$ ) and TDU ( $0.2 < \alpha < 0.6$ ) at selected four East Asian  
292 sites. The SSA, ASY, Re and Ri of complex refractive index as a function of  
293 wavelength (440, 675, 870, and 1020 nm) are presented. For all cases, the spectral  
294 behaviors of aerosol optical parameters exhibit similar features, which can be  
295 representative of typical patterns of Asian dust. The SSA values systematically

296 increase with wavelength at 440-675 nm and keep almost neutral or slight increase for  
297 the wavelengths greater than 675 nm, which is consistent with the previous results of  
298 dust aerosols (Dubovik et al., 2002b; Eck et al., 2005; Bi et al., 2011). In contrast, an  
299 opposite pattern is displayed by imaginary part of refractive index, namely, Ri values  
300 dramatically decrease from 440 nm to 675 nm, and preserve invariant from 675 nm to  
301 1020 nm. These variations indicate that Asian dust aerosols have got much stronger  
302 absorptive ability at shorter wavelength. Alfaro et al. (2004) implied that the  
303 absorption capacity of soil dust increase linearly with iron oxide content, and  
304 | estimated SSA at 325 nm (~0.80) is much lower than that at 660 nm (~0.95). Sokolik  
305 and Toon (1999) revealed that ferric iron oxides (e.g., hematite and goethite) are often  
306 internally mixed with clay minerals and result in significant dust absorption in the  
307 UV/visible wavelengths. Hence, the spectral variations of SSA and Ri with  
308 wavelengths are attributable to the domination of coarse-mode dust particles that have  
309 larger light absorption in the blue spectral band as mentioned above. It is worth noting  
310 that spectral ASY values remarkably reduce from 440 nm to 675 nm, and are almost  
311 constant at 675-1020 nm range. This suggests that Asian dust aerosols have much  
312 stronger scattering at 440 nm than other longer visible wavebands, due to the  
313 contribution of coarse mode particles. By contrast, the spectral behavior of Re is not  
314 obvious for PDU and TDU at all sites, and the mean Re values at 440 nm vary  
315 between 1.50 and 1.56. Although there are 18 years continuous AERONET datasets at  
316 Dalanzadgad site, the effective days of PDU and TDU are only 8 and 6 days,  
317 respectively, almost appearing in springtime period. There are no identifiable  
318 differences for dust absorption properties between PDU and TDU cases for  
319 Dalanzadgad, which indicates again that the site is hardly influenced by  
320 anthropogenic pollutants. The spectral discrepancies of optical characteristics between  
321 PDU and TDU at other three sites show much more apparent than Dalanzadgad,  
322 which is ascribed to these regions are not only affected by dust aerosols, but also  
323 including local anthropogenic emissions, for instance, urban-industry, coal fuel  
324 combustion, biomass burning, mobile source emissions, and agricultural dust (Xu et  
325 al., 2004; Xia et al., 2007; Che et al., 2015; Bi et al., 2011; Wang et al., 2015).

326 Figure 4 is the same as Figure 3, but for selected four Central Asian sites. The  
327 wavelength dependencies of PDU and TDU cases at Central Asian sites are consonant  
328 with that of East Asian sites, despite of somewhat different variations of magnitude  
329 and amplitude. This is expected, because the East Asian desert sites are very close to  
330 the Central Asian desert locations and remain similar chemical compositions of dust  
331 aerosols (Wang et al., 2004). The spectral behaviors of dust optical properties for  
332 PDU at Kandahar and IASBS sites are nearly the same as TDU cases, which agrees  
333 well with the consistent variability of occurrence of dust storms. The wavelength  
334 dependency of dust characteristics for PDU at Dushanbe and Karachi presents large  
335 differences with TDU case, which is also likely due to the influence of local  
336 anthropogenic pollutions. Furthermore, the standard deviation of PDU is far less than  
337 that of TDU at all wavelengths, suggesting that the robustness of PDU recognition  
338 method.

339 Particle size distribution is another critical agent for deciding the optical and  
340 radiative properties of dust aerosol. Nakajima et al. (1996) and Dubovik and King  
341 (2000) uncovered that based on the spherical Mie theory, the retrieval errors of  
342 volume size distribution do not exceed 10% for intermediate particle size ( $0.1 \leq r \leq 7$   
343  $\mu\text{m}$ ) and may greatly increase to 35-100% at the edges of size range ( $r < 0.1 \mu\text{m}$  or  $r > 7$   
344  $\mu\text{m}$ ). As mentioned above, a polydisperse, randomly oriented spheroid method is  
345 utilized in this study, which is demonstrated to remove the artificially increased size  
346 distribution of fine particle mode with  $\text{AOD}_{440} \geq 0.4$  and for solar zenith angle  $> 50^\circ$ .  
347 Additionally, the large errors at the edges do not significantly affect the derivation of  
348 the main features of the particle size distribution (concentration, median and effective  
349 radii, etc.), because typical dust aerosol size distributions have low values at the edges  
350 of retrieval size interval (Dubovik et al., 2002a). Figure 5 delineates the overall  
351 average columnar aerosol volume size distributions ( $dV/d\ln r$ ,  $0.05 \mu\text{m} \leq r \leq 15 \mu\text{m}$ ) for  
352 Pure Dust ( $\alpha < 0.2$ ) and Transported Anthropogenic Dust ( $0.2 < \alpha < 0.6$ ) at selected 13  
353 AERONET sites. Corresponding  $\text{AOD}_{440}$  and effective radius of coarse mode ( $r_{\text{coarse}}$ )  
354 in  $\mu\text{m}$  are also shown. It is apparent that the  $dV/d\ln r$  exhibits a typical bimodal  
355 structure and is dominant by coarse mode for PDU and TDU at all sites. The  $dV/d\ln r$

356 peak of coarse mode particle varies dramatically and appears at a radius  $r_{vc} \sim 2.24 \mu\text{m}$   
 357 for all PDU cases and  $r_{vc} \sim 2.0\text{-}3.0 \mu\text{m}$  for TDU cases~~for all PDU and TDU cases,~~  
 358 while the corresponding peak of fine mode particle arises at a radius  $r_{vf} \sim 0.09\text{-}0.12$   
 359  $\mu\text{m}$ . The  $dV/d\ln r$  peak and effective radius ( $r_{\text{coarse}}$ ) of coarse mode particles strikingly  
 360 increase with the increase of AOD ascribed to the intrusion of dust particles. For  
 361 instance, the  $\text{AOD}_{440}$ ,  $dV/d\ln r$  peak values of coarse mode, and  $r_{\text{coarse}}$  for PDU at  
 362 Minqin site are 0.48,  $0.31 \mu\text{m}^3/\mu\text{m}^2$ , and  $1.74 \mu\text{m}$ , respectively, and corresponding  
 363 values are 1.13,  $0.77 \mu\text{m}^3/\mu\text{m}^2$ , and  $1.93 \mu\text{m}$  at Lahore site, as shown in Fig. 5(a). The  
 364 average volume median radii of fine-mode and coarse-mode particles for PDU are  
 365  $0.159 \mu\text{m}$  and  $2.157 \mu\text{m}$ , respectively, and  $0.140 \mu\text{m}$  and  $2.267 \mu\text{m}$  for TDU (see  
 366 Table. 2). The mean volume concentration ratio of coarse mode to fine mode particles  
 367 ( $C_{vc}/C_{vf}$ ) for Pure Dust is about 18 (varying between 11~31) over East and Central  
 368 Asia, which is close to the average of  $\sim 20$  at Dunhuang\_LZU during the spring of  
 369 2012 (Bi et al., 2014), and much less than that over Saharan pure desert domain ( $\sim 50$ )  
 370 (Dubovik et al., 2002b). The  $dV/d\ln r$  peak of coarse mode for TDU is clearly smaller  
 371 than that for PDU, and corresponding mean  $C_{vc}/C_{vf}$  value is 9 ( $\sim 5\text{-}11$ ). We attribute  
 372 the high fractions of coarse-mode particles to high AOD and low Ångström exponent  
 373 values.

374 In this paper, we postulate that Asian dust particles only possess scattering and  
 375 absorption characteristics. And the absorption AOD value (AAOD) at a specific  
 376 wavelength can be obtained from SSA and AOD, namely,  $\text{AAOD}_\lambda = (1 - \text{SSA}_\lambda) \times \text{AOD}_\lambda$ ,  
 377 where  $\lambda$  is the wavelength. Thereby, the corresponding absorption Ångström exponent  
 378 at 440-870 nm (AAE) is calculated from spectral AAOD values by using a log-linear  
 379 fitting algorithm. Figure 6 outlines the total average Ångström exponent ( $\alpha$ ) and  
 380 absorption Ångström exponent at 440-870 nm, volume concentration of coarse mode  
 381 in  $\mu\text{m}^3/\mu\text{m}^2$ , and volume median radius of coarse mode in  $\mu\text{m}$  for TDU ( $0.2 < \alpha < 0.6$ )  
 382 and PDU ( $\alpha < 0.2$ ) at selected AERONET sites. There are very big differences of all  
 383 quantities between PDU and TDU cases, except for some sites (e.g., Dunhuang and  
 384 Minqin). The primary reason is that we only acquire limited datasets of dust days  
 385 during spring time at Dunhuang and Minqin sites, which are hardly affected by other

386 anthropogenic pollutants. The AE values of TDU show remarkable changes among  
387 each site, ranging from 0.24 to 0.44, whereas corresponding values of PDU keep  
388 comparatively slight variations for selected 13 sites (~0.04-0.15). Furthermore, all the  
389 AAE values of PDU are greater than 1.5, ranging between 1.65 and 2.36, and the  
390 AAE of TDU vary from 1.2 to 2.3. We can conclude that the Asian pure dust aerosols  
391 have got AE values smaller than 0.2 and corresponding AAE larger than 1.50, which  
392 is another typical feature distinguishing with other non-dust aerosols. Yang et al.  
393 (2009) attributed the high AAE values of dust aerosol in China to the presence of  
394 ferric oxides. It is evident that volume concentrations of coarse mode for PDU are  
395 significantly higher than TDU case, which is expected for the more coarse-mode  
396 particles in PDU. While the volume median radius of coarse mode for TDU is greater  
397 than PDU case, although there are some smaller values for TDU at Dalanzadgad and  
398 Yulin sites. This is owing to dust particles at these sites usually mix with other  
399 anthropogenic aerosol species and substantially enhance their median radii.

400 Figure 7 characterizes the overall mean optical properties (e.g., SSA, ASY, Re,  
401 and Ri) at 440 nm for selected 13 sites. In general, the absorption capacity of PDU is  
402 less than that for TDU. That is, higher SSA and smaller Ri values for PDU, except for  
403 Dalanzadgad site. A reasonable interpretation is that threshold criterion method for  
404 PDU in this study has effectively eliminated the fine mode aerosols, which are mostly  
405 the much stronger absorbing aerosols (e.g., soot and biomass burning aerosol) over  
406 East and Central Asia but weaker absorbing pollution aerosols (i.e., sulfate and nitrate)  
407 over Dalanzadgad. Wu et al. (2012, 2014) have documented that sulfate and nitrate in  
408 background atmosphere most likely originated directly from surface soil at the north  
409 and south edges of Taklimakan desert and comprised steadily about 4% of dust  
410 particulate matters, which could partially explain our results. Additionally, the overall  
411 mean ASY and Re of PDU are greater than that of TDU, which again verifies that the  
412 Asian pure dust has got much stronger forward scattering ability than the mixture of  
413 Asian dust. Note that the standard deviation of SSA and Ri for PDU is a factor of two  
414 to four lower than those from TDU. And the total average values of SSA, ASY, Re,  
415 and Ri at 550 nm wavelength for Asian PDU are  $0.935\pm 0.014$ ,  $0.742\pm 0.008$ ,

416 1.526±0.029, and 0.00226±0.00056, respectively, while corresponding values are  
417 0.921±0.021, 0.723±0.009, 1.521±0.025, 0.00364±0.0014 for TDU. Yang et al. (2009)  
418 took advantage of various in situ aerosol optical and chemical measurements at  
419 Xianghe, China during the EAST-AIRC campaign, and deduced a refractive index of  
420 1.53-0.0023i at 550 nm of dust aerosol, which is close to the result of PDU in this  
421 study. Nevertheless, the TDU case should be much closer to actual airborne dust  
422 aerosol in the real world. When the elevated dusts over desert source regions are  
423 transported eastward, they generally mix with other chemical species and react  
424 heterogeneously with anthropogenic pollutants, and thus may significantly modify  
425 their chemical composition and microphysical properties (Arimoto et al., 2004).  
426 Recently, Kim et al. (2011) presented that the annual mean SSA, ASY, Re, and Ri of  
427 complex refractive index for nearly pure Saharan dust are 0.944±0.005, 0.752±0.014,  
428 1.498±0.032, and 0.0024±0.0034 at 550 nm, respectively, which are close to our  
429 results of pure Asian dust but exist some differences of quantitative values and  
430 spectral behaviors.

431 Average spectral optical properties (at 440, 675, 870, and 1020 nm) for PDU and  
432 TDU over East and Central Asian regions are tabulated in Table 2. To our knowledge,  
433 this is the first built on Asian dust optical characteristics utilizing multiyear and  
434 multi-site AERONET measurements, which will hopefully improve uncertainties of  
435 Asian dust shortwave radiative forcing in current regional and global climate models.

#### 436 **4. Discussion**

437 Figure 8 describes the mean spectral behaviors of Re, RI, and SSA for Asian Pure  
438 Dust ( $\alpha < 0.2$ ) in this study along with published dust results over various geographical  
439 locations (Carlson and Caverly, 1977 or C77; Patterson et al., 1977 or P77; WMO,  
440 1983; Hess et al., 1998 or OPAC; Dubovik et al., 2002b or Persian Gulf; Alfaro et al.,  
441 2004 or Ulan Buh Desert; Wang et al., 2004 or ADEC; Todd et al., 2007 or T07). It is  
442 well known that a lot of present-day dust models commonly take advantage of the  
443 Optical Properties of Aerosols and Clouds (OPAC, Hess et al., 1998) or World  
444 Meteorological Organization (WMO, 1983) databases. Curves C77 and P77 show the

445 complex refractive index of Saharan dust in Cape Verde Islands, Barbados West  
446 Indies, Tenerife Canary Islands obtained from laboratory analysis by Carlson and  
447 Caverly (1977) and Patterson et al. (1977), respectively. Curve P77 gives one of the  
448 most widely used datasets of  $R_i$  value in the range 300-700 nm. Curve Persian  
449 Gulf(98-00) displays the refractive index and SSA of dust over Bahrain-Persian Gulf  
450 Desert during period of 1998-2000 derived from Dubovik et al. (2002b). Curve T07  
451 shows the optical properties of mineral dust over Bodélé Depression of northern Chad  
452 during 2005 retrieved from Cimel sun photometer by Todd et al. (2007). And the  
453 curves ADEC and Ulan Buh exhibit the dust absorptive properties over  
454 aforementioned Taklimakan Desert and Ulan Buh Desert of northwest China by Wang  
455 et al. (2004) and Alfaro et al. (2004). Figure 8(a) presents that the spectral behaviors  
456 of  $R_e$  have relatively slight variations with values ranging from 1.50-1.56 apart from  
457 T07 that shows lower  $R_e$  values of 1.44-1.47. Todd et al. (2007) utilized Scanning  
458 Electron Microscope (SEM) analysis of airborne dust material and confirmed that the  
459 mineral dust is dominated by fragmented fossil diatoms from the dry lake bed of the  
460 Bodélé Depression, which is to some extent different from the typical desert soil. As  
461 shown in Figure 8(b), wavelength dependences of  $R_i$  exhibit comparably greater  
462 differences in UV wavebands. In mid-visible and near infrared, our results are slightly  
463 larger than Persian Gulf (98-00) and T07 that are retrieved from Cimel sun  
464 photometer, but still comparable. It is very distinct that the absorbing ability of Asian  
465 pure dust ( $\alpha < 0.2$ ) in the whole spectrum range is about a factor of 4 smaller than  
466 current dust models (WMO, 1983; Hess et al., 1998), and is a factor of 2 to 3 lower  
467 than the results from in situ measurements combined with laboratory analysis or  
468 model calculations (Carlson and Caverly, 1977; Patterson et al., 1977; Wang et al.,  
469 2004). Meanwhile, the wavelength dependences of SSA agree well with Persian Gulf  
470 (98-00) and Ulan Buh Desert, but are much higher than OPAC. The discrepancy  
471 increases dramatically with decreasing wavelength. Such big differences of dust  
472 absorption capacity for diverse dust models (OPAC and WMO) and researches will  
473 certainly lead to different radiative impacts on regional or global climate change.

474 Figure 9 draws the aerosol shortwave direct radiative effects (ARF) at the top of



475 atmosphere (TOA), at the surface (SFC), and in the atmospheric layer (ATM) for  
476 Asian Pure Dust ( $\alpha < 0.2$ ) and Transported Anthropogenic Dust ( $0.2 < \alpha < 0.6$ ) acquired  
477 in this study, and corresponding ARF values for OPAC Mineral accumulated (Mineral  
478 acc.) and transported (Mineral tran.) modes are also presented for comparison. We  
479 make use of the Santa Barbara Discrete-ordinate Atmospheric Radiative Transfer  
480 model (SBDART, Ricchiazzi et al., 1998) to calculate the ARF, which has been  
481 proved to be a reliable software code and widely used for simulating plane-parallel  
482 radiative fluxes in the Earth's atmosphere (Halthore et al., 2005; Bi et al., 2013). The  
483 main input parameters of spectral AOD, surface albedo, WVC, and columnar ozone  
484 amount are prescribed to same values (e.g., 0.72, 0.30, 1.0 cm, and 300 DU for input  
485 AOD<sub>440</sub>, surface albedo, WVC, and ozone amount), and the spectral SSA, ASY, Re,  
486 and Ri values are obtained from aforementioned various dust models. It is evident that  
487 Earth's energy budget is modulated and redistributed by different absorbing properties  
488 of mineral dusts. The results indicate that the cooling rate at SFC (negative radiative  
489 forcing) gradually increases with PDU ( $\alpha < 0.2$ ), TDU ( $0.2 < \alpha < 0.6$ ), OPAC Mineral  
490 accumulated and transported dust modes. By contrast, the cooling intensity at TOA  
491 gradually decreases with diverse dust cases, and even becomes positive radiative  
492 forcing for OPAC transported dust mode, with ARF varying from -15.6, -13.8, -6.9,  
493 and +0.24  $\text{Wm}^{-2}$ , respectively. Therefore, the heating intensity in the atmospheric  
494 layer sharply increases from +22.7, +29.5, +46.6, and +58.3  $\text{Wm}^{-2}$ . The heating rate in  
495 ATM for OPAC Mineral (acc. and tran.) modes is about two-fold greater than Asian  
496 dust cases (PDU and TDU). Such large diabatic heating rates might warm the dust  
497 layer, suppress the development of convection under the lower atmosphere, thus exert  
498 profound impacts on the atmospheric dynamical and thermodynamic structures and  
499 cloud formation together with the strength and occurrence frequency of precipitation  
500 (Rosenfeld et al., 2001; Huang et al., 2010a; Creamean et al., 2013). Hence, accurate  
501 and reliable absorbing characteristics of Asian dust should be considered in  
502 present-day regional climate models.

## 503 **5. Summary**

504 In this study, we have proposed two threshold criteria to discriminate two types of  
505 Asian dust: Pure Dust (PDU,  $\alpha < 0.2$ ) and Transported Anthropogenic Dust (TDU,  
506  $0.2 < \alpha < 0.6$ ). ~~PUD-PDU~~ can represent nearly “pure” dust in desert source regions and  
507 decrease disturbance of other non-dust aerosols, which would also exclude some fine  
508 mode of dust particles. The spectral behaviors of TDU exhibit similar variations with  
509 PDU, but show much stronger absorption and weaker scattering than PDU cases.  
510 There are two markedly identifiable characteristics for Asian PDU. (I) spectral SSA  
511 values systematically increase with wavelength from 440 nm to 675 nm and remain  
512 almost neutral or slight increase for the wavelength greater than 675 nm, whereas an  
513 opposite pattern is shown for imaginary part of refractive index. (II) Asian pure dust  
514 aerosols have got AE values smaller than 0.2 and AAE larger than 1.50. Compared  
515 with current common dust models (e.g., OPAC and WMO), Asian dust aerosol has  
516 relatively weak absorption for wavelengths greater than 550 nm ( $SSA \sim 0.96-0.99$ ), but  
517 presents a moderate absorption in the blue spectral range ( $SSA_{440} \sim 0.92-0.93$ ). The  
518 overall average values of SSA, ASY, Re, and Ri at 550 nm wavelength for Asian PDU  
519 are  $0.935 \pm 0.014$ ,  $0.742 \pm 0.008$ ,  $1.526 \pm 0.029$ , and  $0.00226 \pm 0.00056$ , respectively,  
520 while corresponding values are  $0.921 \pm 0.021$ ,  $0.723 \pm 0.009$ ,  $1.521 \pm 0.025$ ,  
521  $0.00364 \pm 0.0014$  for TDU.

522 It should be noted that the definition of anthropogenic dust in this paper is  
523 ambiguous, and TDU here represents more accurately dominant dust mixing with  
524 other anthropogenic aerosols. ~~It is very difficult~~Because it is very difficult to quantify  
525 the anthropogenic contribution due to large uncertainties in defining the  
526 anthropogenic fraction of ambient dust burden (Sokolik et al., 2001; Huang et al.,  
527 2015). Diverse human activities (e.g., agricultural cultivation, desertification,  
528 industrial activity, transportation, and construction in urbanization) in vulnerable  
529 environments might modify the land use and Earth’s surface cover, and would affect  
530 the occurred frequency and intensity of anthropogenic dust. Hence, the optical  
531 features of anthropogenic dust aerosols are dependent on the source regions and  
532 chemical compositions. However, as concluded by Huang et al. (2015), anthropogenic  
533 dust generated by human activities mainly comes from semi-arid and semi-humid

534 regions (Guan et al., 2016) and is generally mixed with other types of aerosols within  
535 the PBL. And we primarily investigated dust aerosols in arid or semi-arid regions over  
536 East and Central Asia, where are somewhat disturbed by human activities. Therefore,  
537 the key optical properties of TDU derived from this study should to some extent  
538 contain the anthropogenic fraction. To fully elucidate exact optical properties of  
539 anthropogenic dust, we need to explore detailed morphology, mineralogy, and  
540 chemical compositions by means of in situ measurements, laboratory analysis, active  
541 and passive remote sensing methods (e.g., multi-wavelength lidar, AEROENT,  
542 MODIS) as well as model calculations.

543

544 *Acknowledgements.* This work was jointly supported by the National Science Foundation of  
545 China (41521004, 41305025, 41575015 and 41405113), the Fundamental Research Funds for the  
546 Central Universities lzujbky-2015-4 and lzujbky-2016-k01, and the China 111 Project (No. B  
547 13045). We thank the GSFC/NASA AERONET group for processing the AERONET data  
548 (<http://aeronet.gsfc.nasa.gov>). The authors would like to express special thanks to the  
549 principal investigators (Hong-Bin Chen, Philippe Goloub, Bernadette Chatenet, Xiao-Ye Zhang,  
550 Laurent Gomes, Sabur F. Abdullaev, and Hamid Khalesifard) and their staff for effort in  
551 establishing and maintaining the instruments at AERONET sites used in this work. We appreciate  
552 the MODIS and TOMS teams for supplying the satellite data. We would also like to thank all  
553 anonymous reviewers for their constructive and insightful comments.

554

## 555 **References**

556 Alam, K., Trautmann, T., and Blaschke, T.: Aerosol optical properties and radiative forcing over  
557 mega-city Karachi, Atmos. Res., 101, 773-782, doi:10.1016/j.atmosres.2011.05.007, 2011.

558 Alfaro, S. C., Lafon, S., Rajot, J. L., Formenti, P., Gaudichet, A., and Maillé, M.: Iron oxides and  
559 light absorption by pure desert dust: An experimental study, J. Geophys. Res., 109, D08208,  
560 doi:10.1029/2003JD004374, 2004.

561 Alizadeh Choobari, O., Zawar-Reza, P., and Sturman, A.: The global distribution of mineral dust  
562 and its impacts on the climate system: A review, Atmos. Res., 138, 152-165,

563 doi:10.1016/j.atmosres.2013.11.007, 2014.

564 Aoki, T., Motoyoshi, H., Kodama, Y., Yasunari, T. J., Sugiura, K., and Kobayashi, H.:  
565 Atmospheric aerosol deposition on snow surfaces and its effect on albedo, SOLA, 2, 13-16,  
566 doi:10.2151/sola.2006-004, 2006.

567 Arimoto, R., X. Y. Zhang, B. J. Huebert, C. H. Kang, D. L. Savoie, J. M. Prospero, S. K. Sage, C.  
568 A. Schloesslin, H. M. Khaing, and S. N. Oh: Chemical composition of atmospheric aerosols  
569 from Zhenbeitai, China, and Gosan, South Korea, during ACE-Asia, J. Geophys. Res., 109,  
570 D19S04, doi:10.1029/2003JD004323, 2004.

571 Bi, J., Huang, J., Fu, Q., Wang, X., Shi, J., Zhang, W., Huang, Z., and Zhang B.: Toward  
572 characterization of the aerosol optical properties over Loess Plateau of Northwestern China, J.  
573 Quant. Spectrosc. Radiat. Transfer., 112, 346-360, doi:10.1016/j.jqsrt.2010.09.006, 2011.

574 Bi, J., Huang, J., Fu, Q., Ge, J., Shi, J., Zhou, T., and Zhang, W.: Field measurement of clear-sky  
575 solar irradiance in Badain Jaran Desert of Northwestern China, J. Quant. Spectrosc. Radiat.  
576 Transf., 122, 194-207, doi:10.1016/j.jqsrt.2012.07.025, 2013.

577 Bi, J., Shi, J., Xie, Y., Liu, Y., Takamura, T., and Khatri, P.: Dust aerosol characteristics and  
578 shortwave radiative impact at a Gobi Desert of Northwest China during the spring of 2012. J.  
579 Meteor. Soc. Jp, 92A, 33-56, DOI:10.2151/jmsj.2014-A03, 2014.

580 Carlson, T. N. and Caverly, R. S.: Radiative characteristics of Saharan dust at solar wavelengths, J.  
581 Geophys. Res., 82(21), 3141-3152, 1977.

582 Chan, C. -C., Chuang, K. -J., Chen, W. -J., Chang, W. -T., Lee, C. -T., and Peng, C. -M.:  
583 Increasing cardiopulmonary emergency visits by long-range transported Asian dust storms in  
584 Taiwan, Environ. Res., 106, 393-400, 2008.

585 Charlson, R. J., Schwartz, S. E., Hales, J. M., Cess, R. D., Coakley Jr., J. A., Hansen, J. E., and  
586 Hofmann, D. J.: Climate forcing by anthropogenic aerosols, Science, 255, 423-430,  
587 doi:10.1126/science.255.5043.423, 1992.

588 [Che, H., Shi, G., Uchiyama, A., Yamazaki, A., Chen, H., Goloub, P., and Zhang, X.:](#)  
589 [Intercomparison between aerosol optical properties by a PREDE skyradiometer and CIMEL](#)  
590 [sunphotometer over Beijing, China, Atmos. Chem. Phys., 8, 3199-3214,](#)  
591 [doi:10.5194/acp-8-3199-2008, 2008.](#)

592 [Che, H., et al.: Instrument calibration and aerosol optical depth validation of the China Aerosol](#)

593 [Remote Sensing Network, J. Geophys. Res., 114, D03206, doi:10.1029/2008JD011030, 2009a.](#)

594 Che, H., Zhang, X., Alfraro, S., Chatenet, B., Gomes, L., and Zhao, J.: Aerosol optical properties  
595 and its radiative forcing over Yulin, China in 2001 and 2002, *Adv. Atmos. Sci.*, 26(3), 564-576,  
596 doi:10.1007/s00376-009-0564-4, 2009b.

597 [Che, H., Wang, Y., Sun, J., Zhang, X., Zhang, X., and Guo, J.: Variation of aerosol optical](#)  
598 [properties over the Taklimakan Desert in China, \*Aerosol Air Qual. Res.\*, 13, 777-785,](#)  
599 [doi:10.4209/aaqr.2012.07.0200, 2013.](#)

600 [Che, H., Xia, X., Zhu, J., Li, Z., Dubovik, O., Holben, B., Goloub, P., Chen, H., Estelles, V.,](#)  
601 [Cuevas-Agulló, E., Blarel, L., Wang, H., Zhao, H., Zhang, X., Wang, Y., Sun, J., Tao, R., Zhang,](#)  
602 [X., and Shi, G.: Column aerosol optical properties and aerosol radiative forcing during a serious](#)  
603 [haze-fog month over North China Plain in 2013 based on ground-based sunphotometer](#)  
604 [measurements, \*Atmos. Chem. Phys.\*, 14, 2125-2138, doi:10.5194/acp-14-2125-2014, 2014.](#)

605 Che, H., Zhang, X.-Y., Xia, X., Goloub, P., Holben, B., Zhao, H., Wang, Y., Zhang, X.-C., Wang,  
606 H., Blarel, L., Damiri, B., Zhang, R., Deng, X., Ma, Y., Wang, T., Geng, F., Qi, B., Zhu, J., Yu,  
607 J., Chen, Q., and Shi, G.: Ground-based aerosol climatology of China: aerosol optical depths  
608 from the China Aerosol Remote Sensing Network (CARSNET) 2002–2013, *Atmos. Chem.*  
609 *Phys.*, 15, 7619-7652, doi:10.5194/acp-15-7619-2015, 2015.

610 Chin, M., Diehl, T., Dubovik, O., Eck, T. F., Holben, B. N., Sinyuk, A., and Streets, D. G.: Light  
611 absorption by pollution, dust, and biomass burning aerosols: a global model study and  
612 evaluation with AERONET measurements, *Ann. Geophys.*, 27, 3439-3464,  
613 doi:10.5194/angeo-27-3439-2009, 2009.

614 Claquin, T., Schulz, M., Balkanski, Y., and Boucher, O.: Uncertainties in assessing radiative  
615 forcing by mineral dust, *Tellus Ser. B*, 50, 491-505, 1998.

616 Claquin, T., Schulz, M., and Balkanski, Y.: Modeling the mineralogy of atmospheric dust sources,  
617 *J. Geophys. Res.*, 104, D18, 22243-22256, 1999.

618 Creamean, J. M., Suski, K. J., Rosenfeld, D., Cazorla, A., DeMott, P. J., Sullivan, R. C., White, A.  
619 B., Ralph, F. M., Minnis, P., Comstock, J. M., Tomlinson, J. M., and Prather, K. A.: Dust and  
620 biological aerosols from the Sahara and Asia influence precipitation in the western U.S.,  
621 *Science*, 339, 1572-1578, doi:10.1126/science.1227279, 2013.

622 DeMott, P. J., Sassen, K., Poellot, M. R., Baumgardner, D., Rogers, D. C., Brooks, S. D., Prenni,

623 A. J., and Kreidenweis, S. M.: African dust aerosols as atmospheric ice nuclei, *Geophys. Res.*  
624 *Lett.*, 30(14), 1732, doi:10.1029/2003GL017410, 2003.

625 Dubovik, O. and King, M. D.: A flexible inversion algorithm for retrieval of aerosol optical  
626 properties from Sun and sky radiance measurements, *J. Geophys. Res.*, 105(D16),  
627 20673-20696,  
628 doi:10.1029/2000JD900282, 2000.

629 Dubovik, O., Smirnov, A., Holben, B. N., King, M. D., Kaufman, Y. J., Eck, T. F., and Slutsker, I.:  
630 Accuracy assessments of aerosol optical properties retrieved from Aerosol Robotic Network  
631 (AERONET) Sun and sky radiance measurements, *J. Geophys. Res.*, 105(D8), 9791–9806,  
632 doi:10.1029/2000JD900040, 2000.

633 Dubovik, O., Holben, B. N., Lapyonok, T., Sinyuk, A., Mishchenko, M. I., Yang, P., and Slutsker,  
634 I.: Non-spherical aerosol retrieval method employing light scattering by spheroids, *Geophys.*  
635 *Res. Lett.*, 29(10), 1415, doi:10.1029/2001GL014506, 2002a.

636 Dubovik, O., Holben, B. N., Eck, T. F., Smirnov, A., Kaufman, Y. J., King, M. D., Tanré, D., and  
637 Slutsker, I.: Variability of absorption and optical properties of key aerosol types observed in  
638 worldwide locations, *J. Atmos. Sci.*, 59, 590–608, 2002b.

639 Dubovik, O., Sinyuk, A., Lapyonok, T. Holben, B. N., Mishchenko, M., Yang, P., Eck, T. F.,  
640 Volten, H., Muñoz, O., Veihelmann, B., van der Zande, W. J., Leon, J. –F., Sorokin, M., and  
641 Slutsker, I.: Application of spheroid models to account for aerosol particle nonsphericity in  
642 remote sensing of desert dust, *J. Geophys. Res.*, 111, D11208, doi:10.1029/2005JD006619,  
643 2006.

644 Eck, T. F., Holben, B. N., Reid, J. S., Dubovik, O., Smirnov, A., O’Neill, N. T., Slutsker, I., and  
645 Kinne, S.: Wavelength dependence of the optical depth of biomass burning, urban and desert  
646 dust aerosols, *J. Geophys. Res.*, 104, 31 333-31350, 1999.

647 Eck, T. F., et al.: Columnar aerosol optical properties at AERONET sites in central eastern Asia  
648 and aerosol transport to the tropical mid-Pacific, *J. Geophys. Res.*, 110, D06202,  
649 | doi:10.1029/2004JD005274, 2005.

650 Fu, Q., Thorsen, T., Su, J., Ge, J., and Huang, J.: Test of Mie-based single-scattering properties of  
651 non-spherical dust aerosols in radiative flux calculations, *J. Quant. Spectroc. Radiat. Transf.*,  
652 110, 1640-1653, doi:10.1016/j.jqsrt.2009.03.010, 2009.

653 Ge, J., Su, J., Ackerman, T. P., Fu, Q., Huang, J., and Shi, J.: Dust aerosol optical properties  
654 retrieval and radiative forcing over northwest China during the 2008 China-U.S. joint field  
655 experiment, *J. Geophys. Res.*, 115, D00K12, doi:10.1029/2009JD013263, 2010.

656 Ginoux, P., Prospero, J. M., Gill, T. E., Hsu, N. C., and Zhao, M.: Global-scale attribution of  
657 anthropogenic and natural sources and their emission rates based on MODIS Deep Blue aerosol  
658 products, *Rev. Geophys.*, 50, RG3005, doi:10.1029/2012RG000388, 2012.

659 Golitsyn, G. and Gillette, D. A.: Introduction: A joint Soviet-American experiment for the study of  
660 Asian desert dust and its impact on local meteorological conditions and climate, *Atmos.*  
661 *Environ.*, 27A, 16, 2467-2470, 1993.

662 Guan X., Huang, J., Guo, N., Bi, J., and Wang, G.: Variability of soil moisture and its relationship  
663 with surface albedo and soil thermal parameters over the Loess Plateau, *Adv. Atmos. Sci.*, 26(9),  
664 692-700, doi:10.1007/s00376-009-8198-0, 2009.

665 Guan, X., Huang, J., Zhang, Y., Xie, Y., and Liu, J.: The relationship between anthropogenic dust  
666 and population over global semi-arid regions, *Atmos. Chem. Phys.*, 16, 5159-5169,  
667 doi:10.5194/acp-16-5159-2016, 2016.

668 Halthore, R. N., et al.: Intercomparison of shortwave radiative transfer codes and measurements, *J.*  
669 *Geophys. Res.*, 110, D11206, doi:10.1029/2004JD005293, 2005.

670 Hansen, J., Sato, M., and Ruedy, R.: Radiative forcing and climate response, *J. Geophys. Res.*, 102,  
671 6831-6864, 1997.

672 Hess, M., Kopke, P., and Schult, I.: Optical properties of aerosols and clouds: The software  
673 package OPAC, *Bull. Amer. Meteor. Soc.*, 79, 831-844, 1998.

674 Holben, B. N., Eck, T. F., Slutsker, I., Tanre, D., Buis, J. P., Setzer, A., Vermote, E., Reagan, J. A.,  
675 Kaufman, Y. J., Nakajima, T., Lavenu, F., Jankowiak, F., and Smirnov, A., AERONET—A  
676 federated instrument network and data archive for aerosol characterization, *Remote Sens.*  
677 *Environ.*, 66, 1-16, 1998.

678 Huang, J., Minnis, P., Lin, B., Yi, Y., Khaiyer, M. M., Arduini, R. F., Fan, A., and Mace, G. G.:  
679 Advanced retrievals of multilayered cloud properties using multispectral measurements, *J.*  
680 *Geophys. Res.*, 110, D15S18, doi:10.1029/2004JD005101, 2005.

681 Huang, J., Lin, B., Minnis, P., Wang, T., Wang, X., Hu, Y., Yi, Y., and Ayers, J. K.: Satellite-based  
682 assessment of possible dust aerosols semi-direct effect on cloud water path over East Asia,

683 Geophys. Res. Lett., 33, L19802, doi:10.1029/2006GL026561, 2006.

684 Huang, J., Minnis, P., Chen, B., Huang, Z., Liu, Z., Zhang, Q., Yi, Y., and Ayers, J. K.: Long-range  
685 transport and vertical structure of Asian dust from CALIPSO and surface measurements during  
686 PACDEX, *J. Geophys. Res.*, 113, D23212, doi:10.1029/2008JD010620, 2008a.

687 Huang, J., Zhang, W., Zuo, J., Bi, J., Shi, J., Wang, X., Chang, Z., Huang, Z., Yang, S., Zhang, B.,  
688 Wang, G., Feng, G., Yuan, J., Zhang, L., Zuo, H., Wang, S., Fu, C., and Chou, J.: An overview of  
689 the semi-arid climate and environment research observatory over the Loess Plateau, *Adv. Atmos.*  
690 *Sci.*, 25, 906-921, doi:10.1007/s00376-008-0906-7, 2008b.

691 Huang, J., Fu, Q., Su, J., Tang, Q., Minnis, P., Hu, Y., Yi, Y., and Zhao, Q.: Taklimakan dust  
692 aerosol radiative heating derived from CALIPSO observations using the Fu-Liou radiation  
693 model with CERES constraints, *Atmos. Chem. Phys.*, 9, 4011-4021,  
694 doi:10.5194/acp-9-4011-2009, 2009.

695 Huang, J., Minnis, P., Yan, H., Yi, Y., Chen, B., Zhang, L., and Ayers, J. K.: Dust aerosol effect on  
696 semi-arid climate over Northwest China detected from A-Train satellite measurements, *Atmos.*  
697 *Chem. Phys.*, 10, 6863-6872, doi:10.5194/acp-10-6863-2010, 2010a.

698 Huang, J., Fu, Q., Zhang, W., Wang, X., Zhang, R., Ye, H., and Warren, S. G.: Dust and black  
699 carbon in seasonal snow across northern China, *Bull. Amer. Meteor. Soc.*, 92, 175-181,  
700 doi:10.1175/2010BAMS3064.1, 2011.

701 Huang, J., Wang, T., Wang, W., Li, Z., and Yan, H.: Climate effects of dust aerosols over East  
702 Asian arid and semiarid regions, *J. Geophys. Res.*, 119, 11398-11416,  
703 doi:10.1002/2014JD021796, 2014.

704 Huang, J. P., Liu, J. J., Chen, B., and Nasiri, S. L.: Detection of anthropogenic dust using  
705 CALIPSO lidar measurements, *Atmos. Chem. Phys.*, 15, 11653-11665,  
706 doi:10.5194/acp-15-11653-2015, 2015.

707 Huang, J., Yu, H., Guan, X., Wang, G., and Guo, R.: Accelerated dryland expansion under climate  
708 change, *Nature Clim. Change*, 6(2), 166-171, doi:10.1038/nclimate2837, 2016.

709 Huang, Z., Huang, J., Bi, J., Wang, G., Wang, W., Fu, Q., Li, Z., Tsay, S.-C., and Shi, J.: Dust  
710 aerosol vertical structure measurements using three MPL lidars during 2008 China-U.S. joint  
711 dust field experiment, *J. Geophys. Res.*, 115, D00K15, doi:10.1029/2009JD013273, 2010b.

712 Huebert, B. J., Bates, T., Russell, P. B., Shi, G., Kim, Y. J., Kawamura, K., Carmichael, G., and



713 Nakajima, T.: An overview of ACE-Asia: Strategies for quantifying the relationships between  
714 Asian aerosols and their climatic impacts, *J. Geophys. Res.*, 108(D23), 8633,  
715 doi:10.1029/2003JD003550, 2003.

716 Husar, R. B., Tratt, D. M., and Schichtel, B. A., et al.: Asian dust events of April 1998, *J. Geophys.*  
717 *Res.*, 106, D16, 18317-18330, 2001.

718 Jickells, T., An, Z., Andersen, K., Baker, A., Bergametti, G., Brooks, N., Cao, J., Boyd, P., Duce,  
719 R., Hunter, K., Kawahata, H., Kubilay, N., laRoche, J., Liss, P., Mahowald, N., Prospero, J.,  
720 Ridgwell, A., Tegen, I., and Torres, R.: Global iron connections between desert dust, ocean  
721 biogeochemistry, and climate, *Science*, 308, 67-71, doi:10.1126/science.1105959, 2005.

722 Kim, D.-H., Sohn, B. -J., Nakajima, T., Takamura, T., Takemura, T., Choi, B. -C., and Yoon, S. -C.:  
723 Aerosol optical properties over east Asia determined from ground-based sky radiation  
724 measurements, *J. Geophys. Res.*, 109, D02209, doi:10.1029/2003JD003387, 2004.

725 Kim, D., Chin, M., Yu, H., Eck, T. F., Sinyuk, A., Smirnov, A., and Holben, B. N.: Dust optical  
726 properties over North Africa and Arabian Peninsula derived from the AERONET dataset, *Atmos.*  
727 *Chem. Phys.*, 11, 10733-10741, doi:10.5194/acp-11-10733-2011, 2011.

728 Kinne, S., Schulz, M., Textor, C., Guibert, S., Balkanski, Y., Bauer, S. E., Berntsen, T., Berglen, T.  
729 F., Boucher, O., Chin, M., Collins, W., Dentener, F., Diehl, T., Easter, R., Feichter, J., Fillmore,  
730 D., Ghan, S., Ginoux, P., Gong, S., Grini, A., Hendricks, J., Herzog, M., Horowitz, L., Isaksen,  
731 I., Iversen, T., Kirkevåg, A., Kloster, S., Koch, D., Kristjansson, J. E., Krol, M., Lauer, A.,  
732 Lamarque, J. F., Lesins, G., Liu, X., Lohmann, U., Montanaro, V., Myhre, G., Penner, J., Pitari,  
733 G., Reddy, S., Seland, O., Stier, P., Takemura, T., and Tie, X.: An AeroCom initial assessment –  
734 optical properties in aerosol component modules of global models, *Atmos. Chem. Phys.*, 6,  
735 1815-1834, doi:10.5194/acp-6-1815-2006, 2006.

736 Lafon, S., Rajot, J.-L., Alfaro, S. C., and Gaudichet, A.: Quantification of iron oxides in desert  
737 aerosol, *Atmos. Environ.*, 38, 1211-1218, 2004.

738 Lafon, S., Sokolik, I. N., Rajot, J. L., Caquineau, S., and Gaudichet, A.: Characterization of iron  
739 oxides in mineral dust aerosols: Implications for light absorption, *J. Geophys. Res.*, 111,  
740 D21207, doi:10.1029/2005JD007016, 2006.

741 Li, Z., Li, C., Chen, H., Tsay, S.-C., Holben, B., Huang, J., Li, B., Maring, H., Qian, Y., Shi, G.,  
742 Xia, X., Yin, Y., Zheng, Y., and Zhuang, G.: East Asian Studies of Tropospheric Aerosols and

743 their Impact on Regional Climate (EAST-AIRC): An overview, *J. Geophys. Res.*, 116, D00K34,  
744 doi:10.1029/2010JD015257, 2011.

745 Mikami, M., Shi, G. Y., Uno, I., Yabuki, S., Iwasaka, Y., Yasui, M., Aoki, T., Tanaka, T. Y.,  
746 Kurosaki, Y., Masuda, K., Uchiyama, A., Matsuki, A., Sakai, T., Takemi, T., Nakawo, M., Seino,  
747 N., Ishizuka, M., Satake, S., Fujita, K., Hara, Y., Kai, K., Kanayama, S., Hayashi, M., Du, M.,  
748 Kanai, Y., Yamada, Y., Zhang, X. Y., Shen, Z., Zhou, H., Abe, Q., Nagai, T., Tsutsumi, Y., Chiba,  
749 M., and Suzuki, J.: Aeolian dust experiment on climate impact: An overview of Japan-China  
750 joint project ADEC, *Global Planet. Change*, 52, 142-172, doi:10.1016/j.gloplacha.2006.03.001,  
751 2006.

752 Morman, S. A. and Plumlee, G. S.: The role of airborne mineral dusts in human disease, *Aeolian*  
753 *Res.*, 9, 203-212, 2013.

754 Nakajima, T., Tonna, G., Rao, R., Boi, P., Kaufman, Y., and Holben, B.: Use of sky brightness  
755 measurements from ground for remote sensing of particulate polydispersions, *Appl. Opt.*,  
756 35(15), 2672-2686, doi:10.1364/AO.35.002672, 1996.

757 Nakajima, T., Sekiguchi, M., Takemura, T., Uno, I., Higurashi, A., Kim, D., Sohn, B. J., Oh, S. -N.,  
758 Nakajima, T. Y., Ohta, S., Okada, I., Takamura, T., and Kawamoto, K.: Significance of direct and  
759 indirect radiative forcings of aerosols in the East China Sea region, *J. Geophys. Res.*, 108(D23),  
760 8658, doi:10.1029/2002JD003261, 2003.

761 Okin, G. S., Mahowald, N., Chadwick, O. A., and Artaxo, P.: Impact of desert dust on the  
762 biogeochemistry of phosphorus in terrestrial ecosystems, *Global Biogeochem. Cycles*, 18,  
763 GB2005, doi:10.1029/2003GB002145, 2004.

764 Pandithurai, G., Dipu, S., Dani, K. K., Tiwari, S., Bisht, D. S., Devara, P. C. S., and Pinker, R. T.:  
765 Aerosol radiative forcing during dust events over New Delhi, India, *J. Geophys. Res.*, 113,  
766 D13209, doi:10.1029/2008JD009804, 2008.

767 Patterson, E. M., Gillette, D. A., and Stockton, B.: Complex index of refraction between 300 and  
768 700 nm for Saharan aerosols, *J. Geophys. Res.*, 82(21), 3153-3160, 1977.

769 Perlwitz, J., Tegen, I., and Miller, R. L.: Interactive soil dust aerosol model in GISS GCM, 1.  
770 Sensitivity of the soil dust cycle to radiative properties of soil dust aerosols, *J. Geophys. Res.*,  
771 106, D16, 18167-18192, 2001.

772 Prospero, J. M., Ginoux, P., Torres, O., Nicholson, S. E., and Gill, T. E.: Environmental

773 characterization of global sources of atmospheric soil dust identified with the Nimbus 7 total  
774 ozone mapping spectrometer (TOMS) absorbing aerosol product, *Rev. Geophys.*, 40(1), 1002,  
775 doi:10.1029/2000RG000095, 2002.

776 Ramanathan, V., Crutzen, P. J., Kiehl, J. T., and Rosenfeld, D.: Aerosols, climate, and the  
777 hydrological cycle, *Science*, 294, 2119-2124, doi:10.1126/science.1064034, 2001.

778 Ricchiazzi, P., Yang, S., Gautier, C., and Soble, D.: SBDART: A research and teaching software  
779 tool for plane-parallel radiative transfer in the Earth's atmosphere, *Bull. Amer. Meteor. Soc.*, 79,  
780 2101-2114, 1998.

781 Rosenfeld, D., Rudich, Y., and Lahav, R.: Desert dust suppressing precipitation: A possible  
782 desertification feedback loop, *Proc. Natl. Acad. Sci. U.S.A.*, 98, 5975-5980, 2001.

783 Shao, Y., Wyrwoll, K.-H., Chappel, A., Huang, J., Lin, Z., McTainsh, G., Mikami, M., Tanaka, T.,  
784 Wang, X., and Yoon, S.: Dust cycle: An emerging core theme in Earth system science, *Aeolian*  
785 *Res.*, 2, 181-204, 2011.

786 Shen, Z., Sun, J., Cao, J., Zhang, L., Zhang, Q., Lei, Y., Gao, J., Huang, R., Liu, S., Huang, Y.,  
787 Zhu, C., Xu, H., Zheng, C., Liu, P., and Xue, Z.: Chemical profiles of urban fugitive dust PM<sub>2.5</sub>  
788 samples in Northern Chinese cities, *Sci. Total Environ.*, 569-570, 619-626,  
789 doi:10.1016/j.scitotenv.2016.06.156, 2016.

790 Smirnov, A., Holben, B. N., Eck, T. F., Dubovik, O., and Slutsker, I.: Cloud screening and quality  
791 control algorithms for the AERONET database, *Remote Sens. Environ.*, 73, 337-349, 2000.

792 Smirnov, A., Holben, B. N., Kaufman, Y. J., Dubovik, O., Eck, T. F., Slutsker, I., Pietras, C., and  
793 Halthore, R.: Optical properties of atmospheric aerosol in maritime environments, *J. Atmos.*  
794 *Sci.*, 59, 501-523, 2002.

795 Sokolik, I. N. and Golitsyn, G.: Investigation of optical and radiative properties of atmospheric  
796 dust aerosols, *Atmos. Environ.*, 27A, 16, 2509-2517, 1993.

797 Sokolik, I. N. and Toon, O. B.: Incorporation of mineralogical composition into models of the  
798 radiative properties of mineral aerosol from UV to IR wavelengths, *J. Geophys. Res.*, 104, D8,  
799 9423-9444, 1999.

800 Sokolik, I. N., Winker, D. M., Bergametti, G., Gillette, D. A., Garmichael, G., Kaufman, Y. J.,  
801 Gomes, L., Schuetz, L., and Penner, J. E.: Introduction to special section: Outstanding problems  
802 in quantifying the radiative impacts of mineral dust, *J. Geophys. Res.*, 106, D16, 18015-18027,

803 2001.

804 Takamura, T., Nakajima, T., and SKYNET community group: Overview of SKYNET and its  
805 Activities, *Opt. Puray Apl.*, 37, 3303-3308, 2004.

806 Tegen, I. and Fung, I.: Contribution to the atmospheric mineral aerosol load from land surface  
807 modification, *J. Geophys. Res.*, 100, 18707-18726, doi:10.1029/95JD02051, 1995.

808 Todd, M. C., Washington, R., Martins, J. V., Dubovik, O., Lizcano, G., M'Bainayel, S., and  
809 Engelstaedter, S.: Mineral dust emission from the Bodélé Depression, northern Chad, during  
810 BoDEx 2005, *J. Geophys. Res.*, 112, D06207, doi:10.1029/2006JD007170, 2007.

811 Uchiyama, A., Yamazaki, A., Togawa, H., Asano, J., and Shi, G.-Y.: Single scattering albedo of  
812 Aeolian dust as inferred from sky-radiometer and in situ ground-based measurement, *SOLA*,  
813 Vol. 1, pp. 209-212, doi:10.2151/sola.2005-054, 2005.

814 Uno, I., Eguchi, K., Yumimoto, K., Takemura, T., Shimizu, A., Uematsu, M., Liu, Z., Wang, Z.,  
815 Hara, Y., and Sugimoto, N.: Asian dust transported one full circuit around the globe, *Nature*  
816 *Geosci.*, 2, 557-560, doi:10.1038/NGEO583, 2009.

817 Uno, I., Eguchi, K., Yumimoto, K., Liu, Z., Hara, Y., Sugimoto, N., Shimizu, A., and Takemura, T.:  
818 Large Asian dust layers continuously reached North America in April 2010, *Atmos. Chem.*  
819 *Phys.*, 11, 7333-7341, 2011.

820 Wang, G., Huang, J., Guo, W., Zuo, J., Wang, J., Bi, J., Huang, Z., and Shi, J.: Observation  
821 analysis of land-atmosphere interactions over the Loess Plateau of northwest China, *J. Geophys.*  
822 *Res.*, 115, D00K17, doi:10.1029/2009JD013372, 2010a.

823 Wang, H., Shi, G. Y., Aoki, T., Wang, B., and Zhao, T. L.: Radiative forcing due to dust aerosol  
824 over east Asia-north Pacific region during spring, 2001, *Chin. Sci. Bull.*, 49(20): 2212-2219,  
825 2004.

826 Wang, H., Zhang, X., Gong, S., Chen, Y., Shi, G., and Li, W.: Radiative feedback of dust aerosols  
827 on the East Asian dust storms, *J. Geophys. Res.*, 115, D23214, doi:10.1029/2009JD013430,  
828 2010b.

829 Wang, W., Huang, J., Minnis, P., Hu, Y., Li, J., Huang, Z., Ayers, J. K., and Wang, T.: Dusty cloud  
830 properties and radiative forcing over dust source and downwind regions derived from A-Train  
831 data during the Pacific Dust Experiment, *J. Geophys. Res.*, 115, D00H35,  
832 doi:10.1029/2010JD014109, 2010c.

833 Wang, X., Huang, J., Ji, M., and Higuchi, K.: Variability of East Asia dust events and their  
834 long-term trend, *Atmos. Environ.*, 42, 13, 3156-3165, doi:10.1016/j.atmosenv.2007.07.046,  
835 2008.

836 Wang, X., Doherty, S. J., and Huang, J.: Black carbon and other light-absorbing impurities in  
837 snow across Northern China, *J. Geophys. Res.*, 118, 1471-1492, doi:10.1029/2012JD018291,  
838 2013.

839 Wang, X., Pu, W., Shi, J., Bi, J., Zhou, T., Zhang, X., and Ren, Y.: A comparison of the physical  
840 and optical properties of anthropogenic air pollutants and mineral dust over Northwest China, *J.*  
841 *Meteorol. Res.*, 29, 180-200, doi:10.1007/s13351-015-4092-0, 2015.

842 Wang, Y., Wang, R., Ming, J., Liu, G., Chen, T., Liu, X., Liu, H., Zhen, Y., and Cheng, G.: Effects  
843 of dust storm events on weekly clinic visits related to pulmonary tuberculosis disease in Minqin,  
844 China, *Atmos. Environ.*, 127, 205-212, 2016.

845 World Meteorological Organization (WMO), Report of the Experts Meeting on Aerosols and Their  
846 Climatic Effects, WCP-55, Geneva, Switzerland, 1983.

847 Wu, F., D. Zhang, J. Cao, H. Xu, and Z. An: Soil-derived sulfate in atmospheric dust particles at  
848 Taklimakan desert, *Geophys. Res. Lett.*, 39, L24803, doi:10.1029/2012GL054406, 2012.

849 Wu, F., D. Zhang, J. Cao, T. Zhang, and Z. An: Background-like nitrate in desert air, *Atmos.*  
850 *Environ.*, 84, 39-43, 2014.

851 Xia, X., Chen, H., Goloub, P., Zhang, W., Chatenet, B., and Wang, P.: A compilation of aerosol  
852 optical properties and calculation of direct radiative forcing over an urban region in northern  
853 China, *J. Geophys. Res.*, 112, D12203, doi:10.1029/2006JD008119, 2007.

854 Xu, J., Bergin, M. H., Greenwald, R., Schauer, J. J., Shafer, M. M., Jaffrezo, J. L., and Aymoz, G.:  
855 Aerosol chemical, physical, and radiative characteristics near a desert source region of  
856 northwest China during ACE-Asia, *J. Geophys. Res.*, 109, D19S03, doi:10.1029/2003JD004239,  
857 2004.

858 Yang, M., Howell, S. G., Zhuang, J., and Huebert, B. J.: Attribution of aerosol light absorption to  
859 black carbon, brown carbon, and dust in China—interpretations of atmospheric measurements  
860 during EAST-AIRE, *Atmos. Chem. Phys.*, 9, 2035-2050, doi:10.5194/acp-9-2035-2009, 2009.

861 Zhang, X., Arimoto, R., and An, Z.: Dust emission from Chinese desert sources linked to  
862 variations in atmospheric circulation, *J. Geophys. Res.*, 102, D23, 28041-28047,

863 doi:10.1029/97JD02300, 1997.

864 Zheng, Z., Ren, H., and Huang, J.: Analogue correction of errors based on seasonal climatic

865 predictable components and numerical experiments, *Acta Physica Sinica*, 58(10), 7359-7367,

866 2009.

867

## 868 **Figure captions**

869

870 **Table 1.** Overall average and standard deviation of key optical properties at 550 nm (e.g.,  
871 single-scattering albedo, asymmetry factor, real part and imaginary part of complex refractive  
872 index) for Asian pure Dust (PDU). Ångström wavelength exponent ( $\alpha$ ) is in the range of 440-870  
873 nm. Minimum and maximum values of the optical properties are in parenthesis for each  
874 corresponding column. Measuring period and the total number of PDU ( $\alpha < 0.2$ ) and Transported  
875 Anthropogenic Dust (TDU,  $0.2 < \alpha < 0.6$ ) days are in the parenthesis for the first and last column,  
876 respectively.

Site (sampled period)	SSA (min, max)	ASY (min, max)	Re (min, max)	Ri ( $\times 10^{-3}$ )	Ångström (440-870 nm)	PDU/days (TDU)
SACOL (2006-2012)	0.932±0.018 (0.888, 0.971)	0.741±0.012 (0.715, 0.771)	1.534±0.044 (1.438, 1.60)	2.251±0.788 (0.913, 5.51)	0.120±0.049 (0.0, 0.198)	38 (97)
Dalanzadgad (1997-2014)	0.930±0.012 (0.912, 0.949)	0.746±0.010 (0.724, 0.766)	1.512±0.046 (1.447, 1.60)	2.407±0.414 (1.649, 3.19)	0.127±0.079 (-0.06, 0.199)	8 (6)
Beijing (2001-2015)	0.917±0.020 (0.863, 0.963)	0.742±0.012 (0.716, 0.769)	1.557±0.043 (1.401, 1.60)	2.801±0.865 (1.032, 6.20)	0.117±0.067 (-0.048, 0.199)	46 (67)
Yulin (2001-2002)	0.907±0.024 (0.863, 0.952)	0.748±0.010 (0.731, 0.771)	1.559±0.038 (1.476, 1.60)	3.564±1.589 (1.370, 7.92)	0.077±0.068 (-0.024, 0.188)	13 (16)
Dushanbe (2010-2015)	0.941±0.012 (0.916, 0.959)	0.739±0.011 (0.710, 0.765)	1.529±0.041 (1.436, 1.60)	2.011±0.551 (1.022, 3.475)	0.128±0.054 (-0.02, 0.198)	26 (95)
Karachi (2006-2014)	0.945±0.012 (0.916, 0.977)	0.741±0.011 (0.714, 0.767)	1.518±0.030 (1.449, 1.60)	1.938±0.561 (0.758, 3.439)	0.141±0.041 (-0.005, 0.20)	83 (286)
Lahore (2007-2015)	0.930±0.014 (0.901, 0.957)	0.740±0.010 (0.721, 0.765)	1.519±0.038 (1.432, 1.60)	2.253±0.611 (1.207, 3.623)	0.136±0.052 (0.023, 0.198)	26 (248)
IASBS (2010-2013)	0.933±0.017 (0.883, 0.958)	0.725±0.011 (0.704, 0.746)	1.572±0.024 (1.525, 1.60)	2.290±0.845 (1.245, 5.029)	0.098±0.050 (0.021, 0.195)	19 (12)
Kandahar (2008/04-06)	0.925±0.013 (0.903, 0.955)	0.729±0.017 (0.700, 0.768)	1.534±0.035 (1.492, 1.60)	2.855±0.775 (1.445, 4.65)	0.147±0.054 (0.00, 0.199)	10 (4)
Dunhuang (2001/03-05)	0.947±0.015 (0.918, 0.970)	0.745±0.013 (0.723, 0.761)	1.547±0.037 (1.494, 1.60)	1.714±0.697 (1.014, 3.14)	0.039±0.029 (-0.003, 0.091)	6 (0)
Dunhuang_LZU (2012/04-05)	0.958±0.007 (0.951, 0.968)	0.741±0.021 (0.707, 0.771)	1.495±0.042 (1.451, 1.580)	1.589±0.292 (1.092, 1.84)	0.153±0.026 (0.117, 0.184)	5 (4)
Inner_Mongolia (2001/04-05)	0.948±0.012 (0.930, 0.960)	0.751±0.006 (0.743, 0.759)	1.499±0.042 (1.426, 1.54)	1.641±0.457 (1.169, 2.45)	0.069±0.054 (0.011, 0.165)	4 (1)

Minqin (2010/05-06)	0.945±0.002 (0.942, 0.947)	0.756±0.014 (0.740, 0.764)	1.469±0.023 (1.449, 1.494)	2.036±0.220 (1.883, 2.29)	0.119±0.023 (0.103, 0.146)	2 (0)
<b>Overall Mean</b>	<b>0.935±0.014</b>	<b>0.742±0.008</b>	<b>1.526±0.029</b>	<b>2.258±0.556</b>	<b>0.113±0.033</b>	<b>PDU</b>
<b>Overall Mean</b>	<b>0.921±0.021</b>	<b>0.723±0.009</b>	<b>1.521±0.025</b>	<b>3.643±1.372</b>	<b>0.355±0.06</b>	<b>TDU</b>

877

878

879

880 **Table 2.** Spectral optical properties of Pure Dust ( $\alpha < 0.2$ ) and Transported Anthropogenic Dust

881 ( $0.2 < \alpha < 0.6$ ) averaged for 13 sites over East and Central Asia areas.

Asian Dust	Pure Dust ( $\alpha < 0.2$ )	Transported Anthropogenic Dust ( $0.2 < \alpha < 0.6$ )
$\omega_0(440/675/870/1020)$	0.906/0.962/0.971/0.975 ±0.009	0.897/0.943/0.954/0.959 ±0.019
$Re(440/675/870/1020)$	1.520/1.533/1.517/1.503 ±0.026	1.509/1.533/1.532/1.525 ±0.027
$Ri(440/675/870/1020) \times 10^{-3}$	3.413/1.574/1.449/1.449 ±0.450	5.064/2.737/2.510/2.486 ±1.300
$ASY(440/675/870/1020)$	0.758/0.727/0.724/0.726 ±0.008	0.736/0.711/0.710/0.712 ±0.009
$r_{Vf}(\mu m); \sigma_f$	0.159±0.029	0.140±0.011
$r_{Vc}(\mu m); \sigma_c$	2.157±0.112	2.267±0.214
$C_{vf}(\mu m^3/\mu m^2)$	0.037±0.011; $0.06 \times \tau(1020) - 0.001$	0.038±0.011; $0.12 \times \tau(1020) - 0.014$
$C_{vc}(\mu m^3/\mu m^2)$	0.632±0.167; $0.88 \times \tau(1020) - 0.07$	0.343±0.084; $0.90 \times \tau(1020) - 0.06$
$C_{vc}/C_{vf}$	17.9 (11~31)	9.1 (5~11)

882 Each variable is accompanied by a standard deviation (e.g., ±0.01).  $r_{Vf}$  and  $r_{Vc}$  are the volume

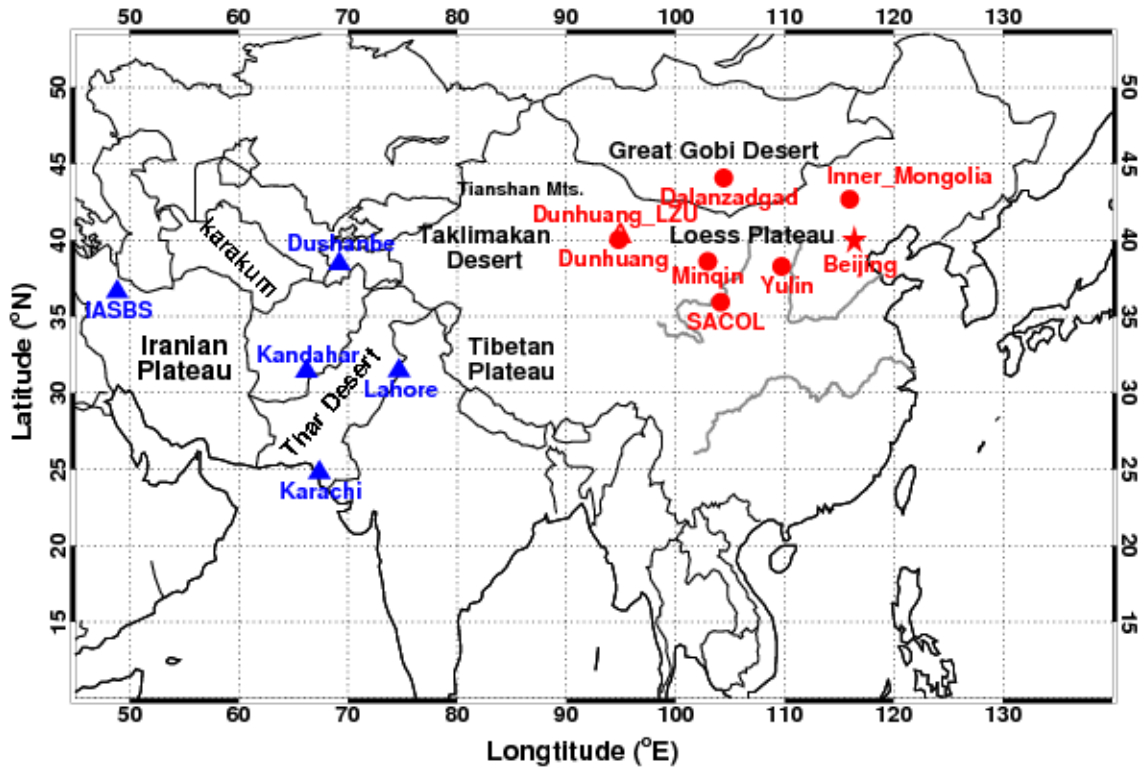
883 median radii of fine-mode and coarse-mode particles in  $\mu m$ ;  $C_{vf}$  and  $C_{vc}$  denote the volume

884 concentrations of fine-mode and coarse-mode particles in  $\mu m^3/\mu m^2$ , respectively. The dynamic

885 dependencies of dust optical properties are exhibited as functions of  $AOD_{1020}$ , with correlation

886 coefficients greater than 0.93 for all cases.

887

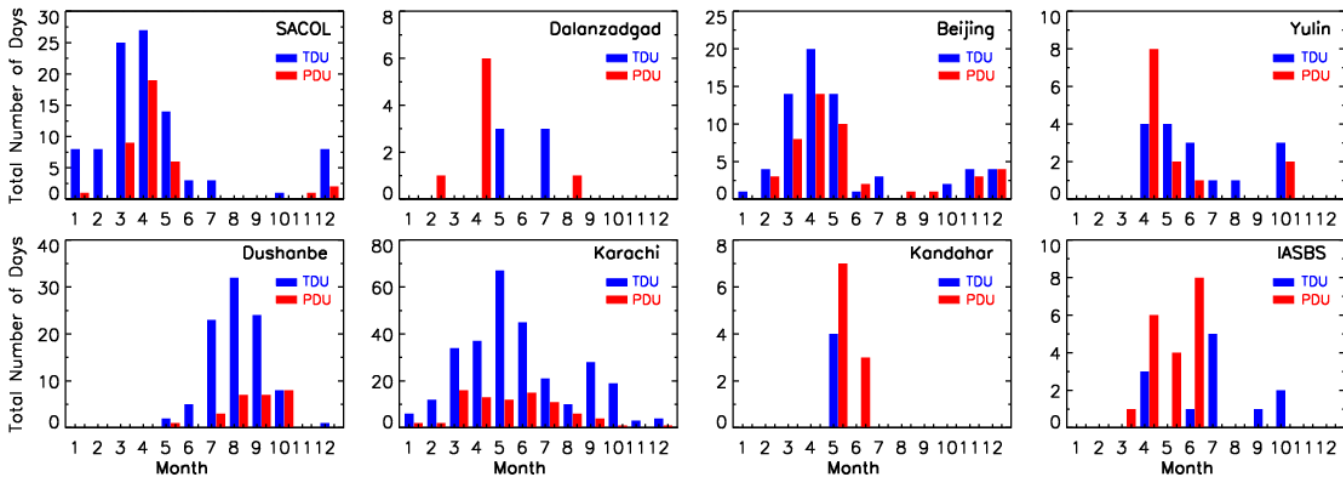


888

889 **Figure 1.** Geographical location of selected 13 AERONET sites in this study. Eight sites over East  
 890 Asian region are labeled with red colors, and five sites over Central Asian region are labeled with  
 891 blue colors. The major Great deserts or Gobi deserts along with plateaus are marked with black  
 892 font.

893

894

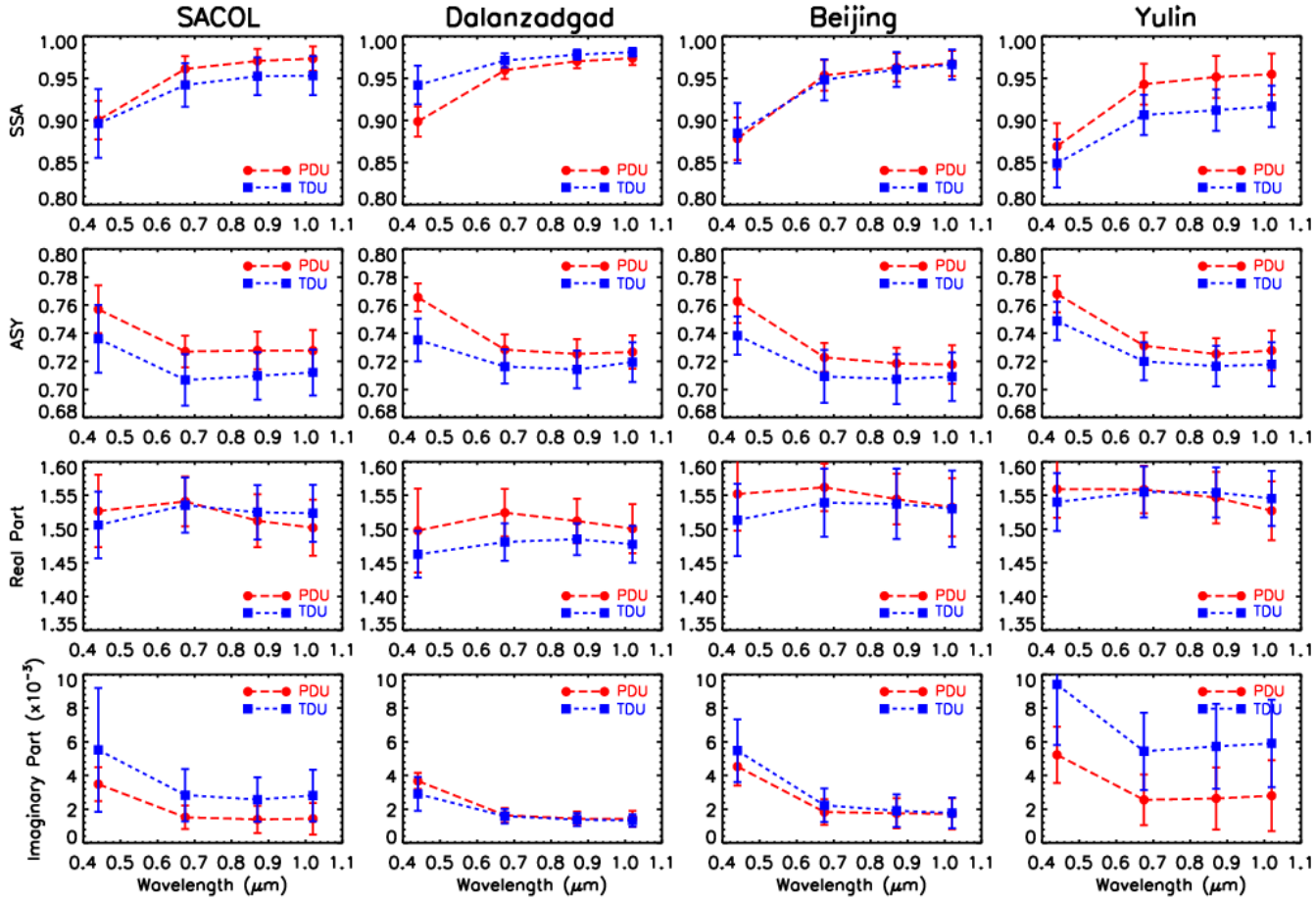


895

896 **Figure 2.** Occurrence frequency of total number days for Pure Dust ( $\alpha < 0.2$ , PDU with red color)  
 897 and Transported Anthropogenic Dust ( $0.2 < \alpha < 0.6$ , TDU with blue color) at selected four East  
 898 Asian sites (top panel) and four Central Asian sites (bottom panel).

899

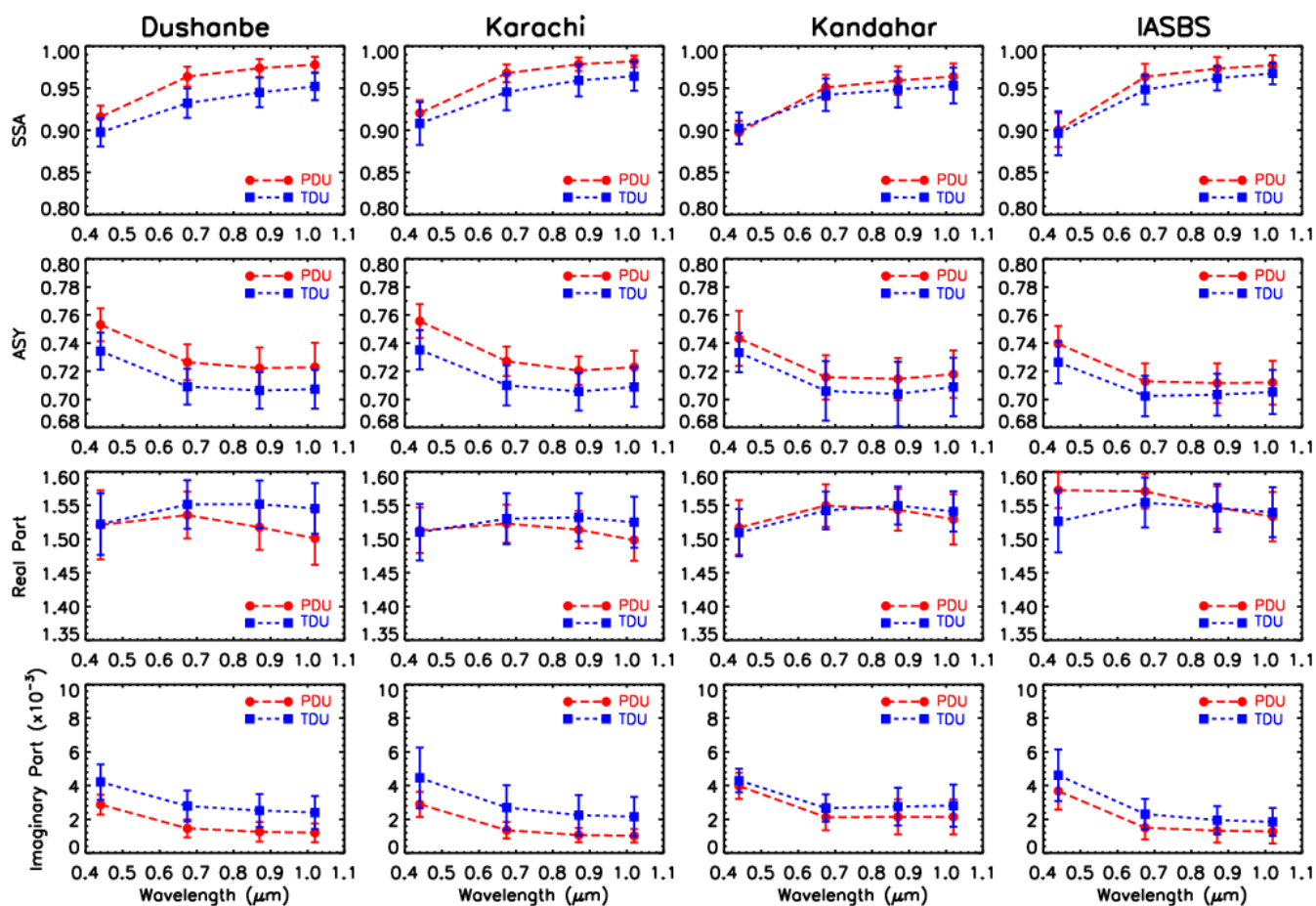




900

901 **Figure 3.** Overall average spectral behavior of key optical properties for Pure Dust ( $\alpha < 0.2$ , PDU  
 902 with red circle) and Transported Anthropogenic Dust ( $0.2 < \alpha < 0.6$ , TDU with blue square) at  
 903 selected four East Asian sites (SACOL, Dalanzadgad, Beijing and Yulin). The error bars indicate  
 904 plus or minus one standard deviation.

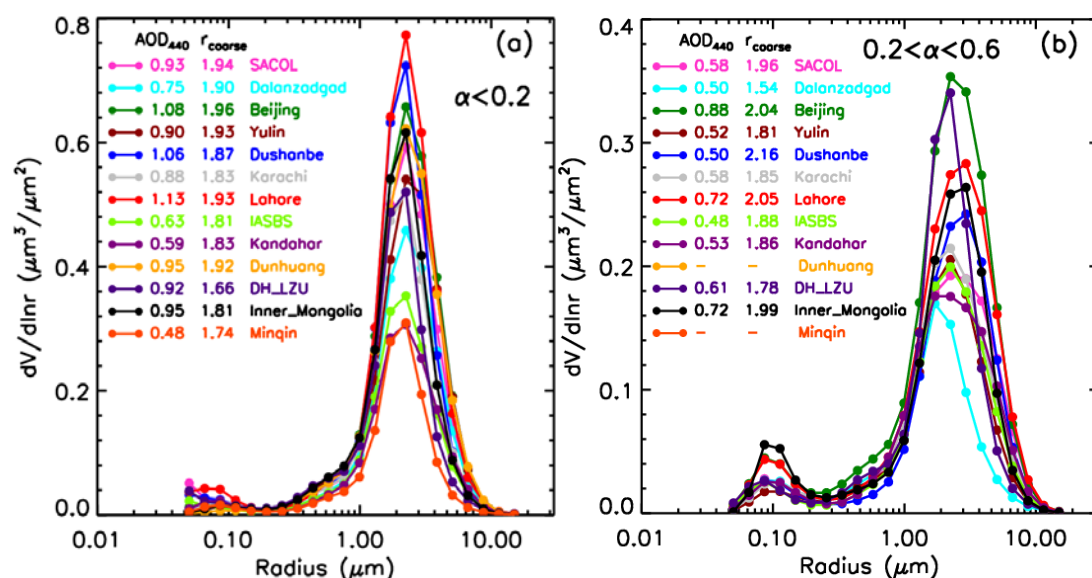
905



906

907 **Figure 4.** The same as Figure 3, but for selected four Central Asian sites (Dushanbe, Karachi,  
 908 Kandahar and IASBS).

909

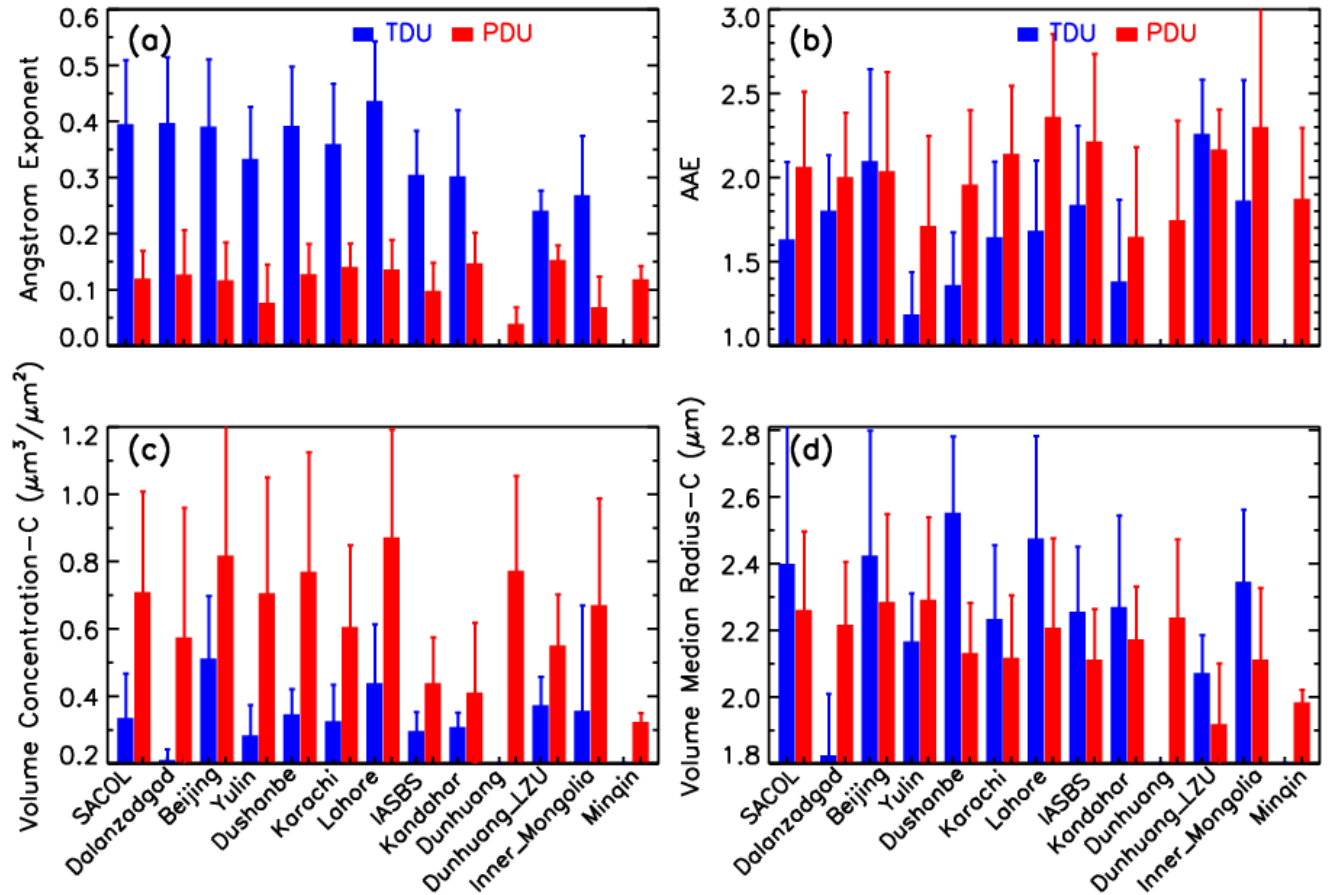


910

911 **Figure 5.** Overall average of aerosol volume size distributions in the entire atmospheric column  
 912 for (a) Pure Dust ( $\alpha < 0.2$ ) and (b) Transported Anthropogenic Dust ( $0.2 < \alpha < 0.6$ ) at selected 13  
 913 AERONET sites. Corresponding aerosol optical depth at 440 nm (AOD<sub>440</sub>) and effective radius of  
 914 coarse mode ( $r_{\text{coarse}}$ ) in  $\mu\text{m}$  are also shown. Note that the “-” in Figure 5(b) represents that

915 | missing data for AOD<sub>440</sub> and r<sub>coarse</sub> at Dunhuang and Minqin sites.

916  
917  
918  
919  
920  
921  
922  
923

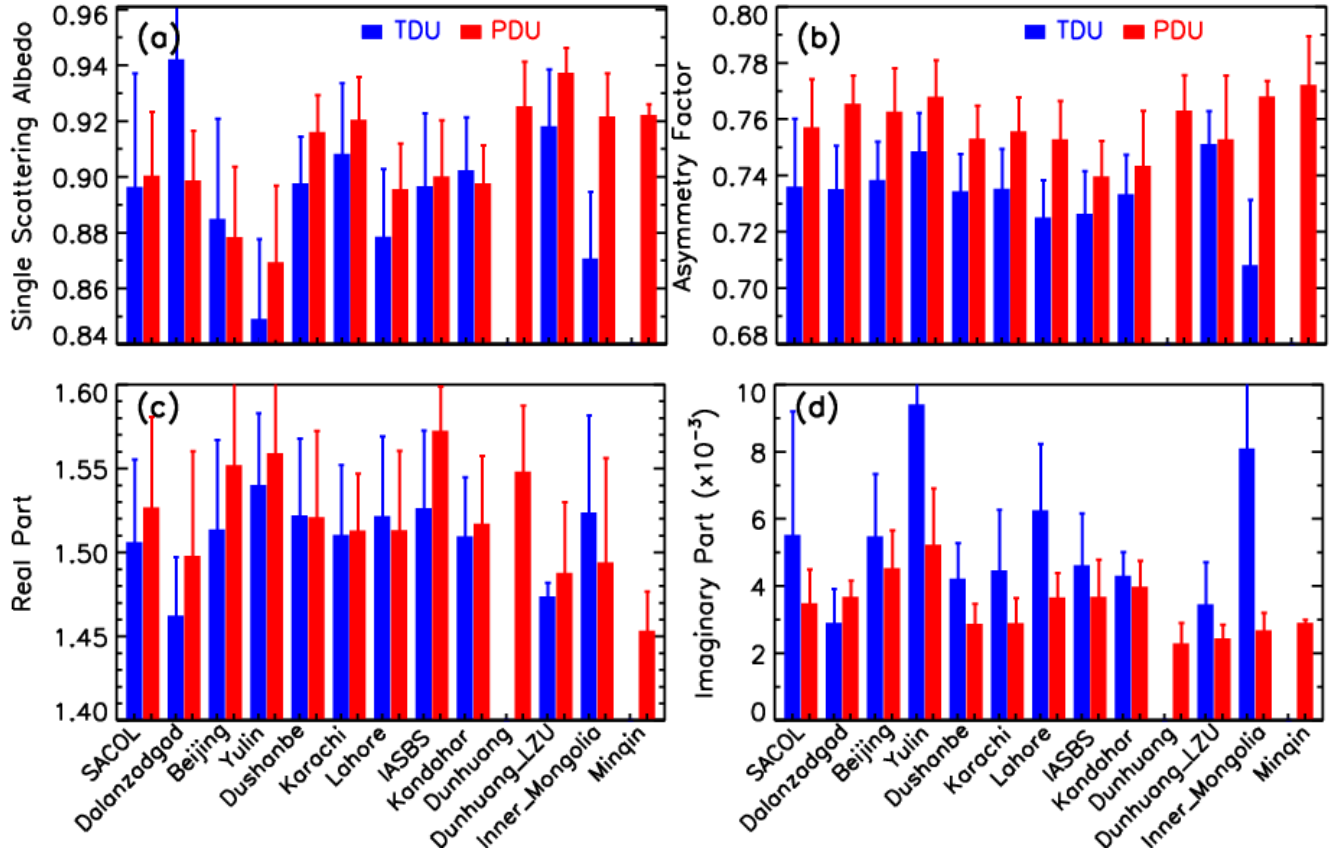


924

925 **Figure 6.** Total average values of (a) Ångström exponent (440-870 nm), (b) absorption Ångström  
926 exponent at 440-870 nm (AAE), (c) volume concentration of coarse mode ( $\mu\text{m}^3/\mu\text{m}^2$ ), and (d)  
927 volume median radius of coarse mode in  $\mu\text{m}$  for Transported Anthropogenic Dust ( $0.2 < \alpha < 0.6$ ,  
928 blue color) and Pure Dust ( $\alpha < 0.2$ , red color) at 13 selected AERONET sites. The error bars  
929 indicate plus or minus one standard deviation.

930  
931  
932  
933  
934  
935  
936  
937

938  
 939  
 940  
 941  
 942  
 943  
 944



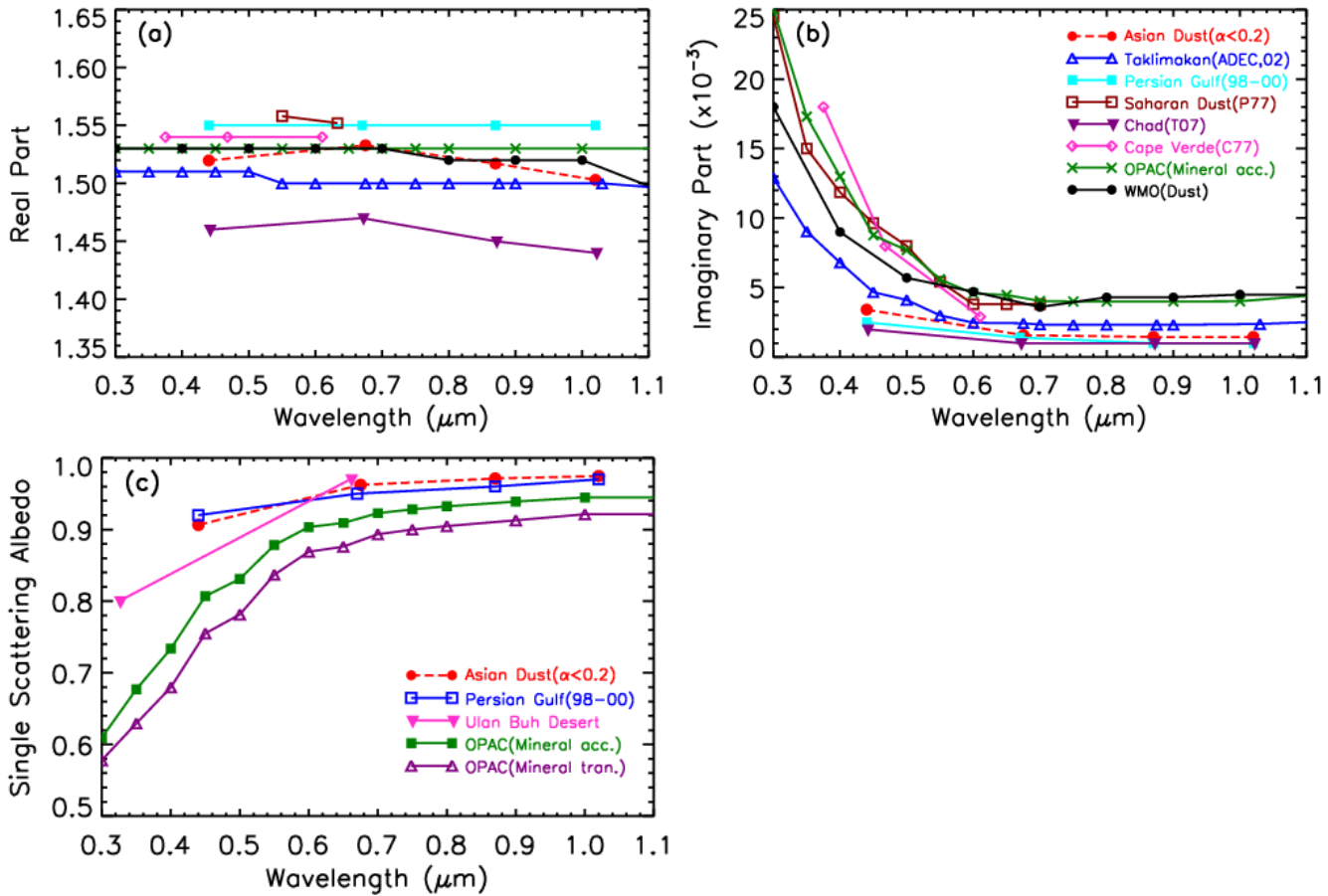
945

946

947 **Figure 7.** The same as Figure 5, but for (a) sing-scattering albedo, (b) asymmetry factor, (c) real  
 948 part and (d) imaginary part of complex refractive index at 440 nm.

949  
 950  
 951  
 952  
 953  
 954  
 955  
 956  
 957  
 958  
 959  
 960  
 961  
 962

963  
 964  
 965  
 966  
 967  
 968  
 969  
 970



971

972

973 **Figure 8.** Mean spectral behaviors of (a) real part, (b) imaginary part of complex refractive index,  
 974 and (c) single-scattering albedo for Asian Pure Dust ( $\alpha < 0.2$ ) calculated for 13 AERONET sites,  
 975 and results of current common dust models (OPAC, WMO), Bahrain-Persian Gulf of Desert dust  
 976 (1998-2000), Saharan dust (Chad, Cape Verde Islands), and Chinese Gobi desert (Taklimakan,  
 977 Ulan Buh Desert) are also shown for comparison.

978

979

980

981

982

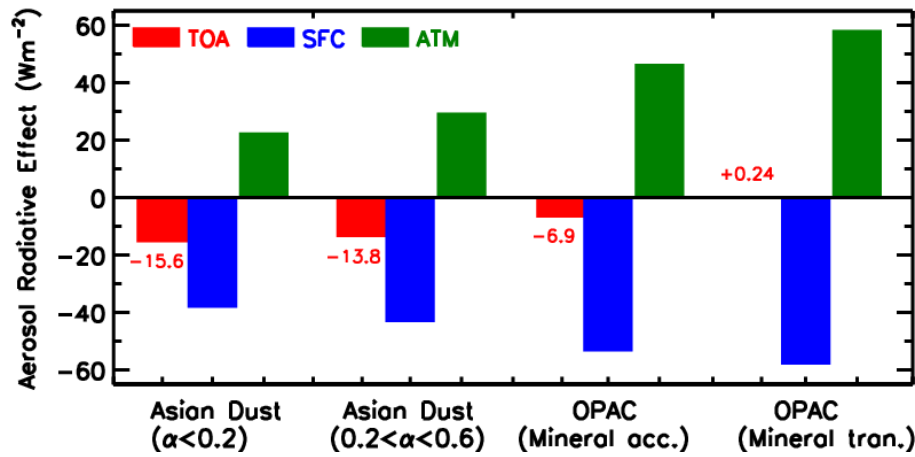
983

984

985

986

987  
988  
989  
990  
991



992  
993  
994  
995  
996  
997

**Figure 9.** Aerosol shortwave direct radiative effects at the top of the atmosphere (TOA, red color), at the surface (SFC, blue color), and in the atmospheric layer (ATM, green color) for Asian Pure Dust ( $\alpha < 0.2$ ) and Transported Anthropogenic Dust ( $0.2 < \alpha < 0.6$ ) computed in this study, and corresponding values for OPAC Mineral accumulated (Mineral acc.) and transported (Mineral tran.) modes are also presented for comparison.